UNIVERSITÀ DEGLI STUDI DI MILANO

PhD course in Veterinary and Animal Science
Class XXXIII

Dipartimento di Medicina Veterinaria

Imaging the sentinel lymph node in small animal oncology

VET/09

PhD Candidate: Martina MANFREDI
R12012

Supervisor: Prof. Davide Danilo ZANI

Coordinator: Prof. Valeria GRIECO

– Academic year 2019/2020 –

Table of Contents

Abstract

Sentinel lymph node (SLN) biopsy has become the cornerstone for tumor staging in patients affected by different solid tumors. To identify the first lymph node draining the tumor site, several mapping modalities have been investigated in human medicine and applied in veterinary oncology, either as experimental models or in clinical setting. In this dissertation, after an extensive literature review, we investigate the principal SLN imaging techniques, such as lymphoscintigraphy, which is considered the gold standard in human oncology, the use of blue dye and computed tomography (CT)-indirect lymphography for SLN mapping in canine patients with spontaneous malignant tumors. The feasibility of Single Proton Emission Computed Tomography (SPECT)/CT images fusion is described for the first time in clinical veterinary oncology. The results of these studies reinforce the paramount importance of SLN mapping incorporation in veterinary practice, supporting the use of combined techniques to increase the SLN detection rate.

1. Literature review

1.1 Lymph node staging

The assessment of lymphatic metastatic spread is a critical component in the staging of malignant tumors, in order to determine the patient prognosis and the choice of treatment. The lymphatic system represents a major route of dissemination for certain cancer types, such as carcinoma and round cell tumors. The thin-walled lymphatic vessels offer little resistance to tumor cell penetration, a high hyaluronic content, and less turbulence than blood vessels, providing a favorable route for cancerous cells to penetrate the lymphatic vessels and invade lymph nodes *(Friedl et al., 2003; Fidler et al., 2003; Ran et al., 2010)*.
In veterinary medicine, the evaluation of regional lymph nodes in oncological patients includes physical examination (i.e., palpation), fine needle aspiration (FNA), needle core biopsy, and excisional biopsy. The assessment of lymph node based on physical examination alone proved to be inaccurate for metastasis detection, as well as sampling the regional lymph nodes only if visibly or palpably enlarged *(Langenbach et al., 2001; Williams et al., 2003)*. Histopathological examination is to be considered the gold standard for identifying lymph node metastasis. A recent study evaluating sensitivity and specificity of FNA for nodal staging in dogs with solid malignant tumors found that cytology sensitivity was lower than histopathology, particularly in cases of sarcoma, mast cell tumor (MCT) and melanoma *(Fournier et al., 2018)*. Furthermore, surgical extirpation of the lymph node removes a potential tumor-harboring site and may thus improve the control over lymphatic cancer dissemination. In veterinary oncology, a possible therapeutic role of regional lymphadenectomy was described in dogs with stage II cutaneous MCT undergoing surgical removal of the primary tumor *(Marconato et al., 2018)*.
Because of the paramount importance of accurate nodal staging, the choice of which lymph node should be removed can be challenging. In fact, besides individual anatomical differences among animals of different breeds, the tumor-induced lymphangiogenesis determines the creation of atypical lymphatic pathways, creating new connections with unexpected lymphatic basins. Cancerous and inflammatory cells of the tumor microenvironment release factors such as vascular endothelial growth factor C and D, which promote lymphatics remodeling and enlargement in and around solid tumors *(Ran et al., 2010; Stacker et al., 2014)*. In 2003, Pereira et al. proved this theory comparing the lymphatic drainage of healthy and neoplastic mammary glands in 46 female dogs. The neoplastic mammary glands presented more types of lymphatic anastomosis than healthy glands, therefore the presence of mammary neoplasia could change the regional lymphatic drainage pattern, recruiting different lymphatic basins *(Pereira et al., 2003)*.

1.2 The Sentinel lymph node concept

The sentinel lymph node (SLN) concept is based on the orderly progression of tumor metastatic cells from peritumoral lymphatics to the regional lymph node, called "*sentinel*". The sentinel lymph node is the first node to receive lymphatic drainage from a primary tumor (first echelon), while the second echelon node receives drainage from a sentinel node.
Therefore, the sentinel node will be the first lymph node to harbor metastasis, and its histopathological examination will accurately predict the involvement of higher echelon nodes and, therefore, the tumor lymphatic spread.
In human literature, the term "sentinel node" was firstly used by Ernest A. Gould (1960) to describe a normal-appearing lymph node, which was reported to be metastatic at histopathological examination, in a patient with a parotid gland carcinoma. The lymph node pathological status guided the decision to perform a radical neck dissection in that patients and also during the following parotidectomy procedures. After few years, Riveros et al. *(Riveros et al., 1967)* described a lymphadenography technique with blue dye (methylene blue and procaine solution) and iodized oil (Lipiodol) to identify tributary lymph nodes in patients with penile cancer. Ten years later, in 1977, Cabanas and colleagues described the sentinel lymph node mapping and biopsy as a recommended part of the oncological staging for penile carcinoma *(Cabanas et al., 1977)*. Since then, numerous studies have been conducted applying the SLN concept to different types of malignancies and, nowadays, SLN biopsy has become the standard of care in the treatment of melanoma, breast, vulvar, and cervical cancer *(Dogan et al., 2019).*
Animal models provided valuable evidences for determining the feasibility of SLN mapping for selective lymphadenectomy *(Wong et al., 1991; Reynolds et al., 1999; Nwogu et al., 2002; Alex et al., 2004)* but was only in 2002 that the SLN concept was introduced in veterinary oncology (*Balogh et al., 2002*) and seven years later, Tuohy and colleagues stated the need to incorporate SLN evaluation into routine veterinary clinical practice *(Tuohy et al., 2009)*.

1.3 Sentinel lymph node mapping

Clinical identification of SLN can be performed through peritumoral injection of different types of tracers, which are collected by lymphatic vessels and lead to the tumor draining lymph node (*Figure 1.1*). Thereafter, labeled SLN are surgically removed and histologically evaluated for the presence of metastasis. Several SLN mapping techniques have been investigated in human medicine and applied in canine and feline patients, either as experimental models or in clinical setting. In the next paragraphs, a brief description of the existing literature on SLN mapping techniques in veterinary medicine will be provided.

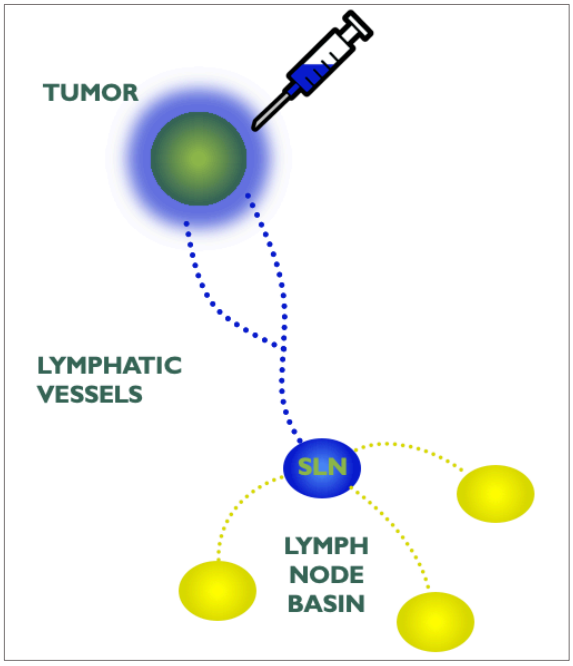

Figure 1.1 The sentinel lymph node mapping procedure. The tracer is injected around the primary tumor, where is collected by lymphatic vessels and drained to the sentinel lymph node.

1.3.1 Vital dyes

The first technique developed for SLN detection was the use of vital colored dyes *(Riveros et al., 1967; Morton et al., 1992)*. The dye is injected peritumorally, where is collected by lymph vessels and drained by the regional lymph node. Therefore, the SLN will be stained by the dye, allowing the direct visualization of lymphatic vessel and lymph nodes by the surgeon, with a faster intraoperative localization. Wong et al. *(1991)* conducted a study to determine the ideal dye among methylene blue, isosulfan blue and Cyalume for lymphatics identification in a feline model. Cyalume, a fluorescent dye, allowed the lymphatics identification but presented substantial problems with leakage into the surrounding interstitial space, while intradermal injection of MB showed poor lymphatic draining and cluttered staining of the surrounding tissue. The most useful dye proved to be isosulfan blue, rapidly entering lymphatics with minimal diffusion into surrounding tissue. Isosulfan blue is a monosodium salt of a 2,5 disulfonated triphenylmethane dye, with two SO_3 groups that bind to proteins, creating a protein-dye complex with affinity for lymphatics *(Mathelin et al., 2009)*. Since then, other triphenylmethane-based dyes were used for SLN mapping, such as patent blue (an ISB structural isomer, also called sulfan blue, food blue 3, patent blue VF, and acid blue 1) and patent blue V (also called patent blue violet, food blue 5, acid blue 3, and disulfine blue) *(Scherern et al., 2006)*. However, triphenylmethane-based dyes appeared to be associated with a significant number of allergic reactions (0.5-2.7%), some of which were life-threatening *(Garbay et al., 2016)*. Methylene blue (MB, *methylthionine hydrochloride*) is a smaller molecule compared to isosulfan blue, with no sulfonic acid groups in its structure and it does

not bind to proteins. Further clinical multicentric studies reported MB to be a safer alternative to triphenylmethane-based dyes, equally effective in SLN detection, although localized reactions, including necrosis of the skin and subcutaneous tissues and necrotic abscesses, have been described *(Mathelin et al., 2009)*.

In veterinary medicine, the use of blue dyes for SLN mapping is less expensive and easily accessible to all practitioners compared to other tracers (i.e., radiopharmaceuticals). In 2006, Wells et al. *(2006)* described a SLN mapping technique using intradermal injection of patent blue violet and fluorescein in healthy dogs. The identification of SLN was accomplished for 98% of the injection sites with no clinical differences between the dyes in the ability to stain lymphatic vessels and nodes. Ten years later, Beserra et al. *(2016)* reported 89.5% sensitivity and 100% specificity for SLN mapping in 41 bitches with mammary carcinoma using solely patent blue V, with a technique accuracy of 95.7%. Nonetheless, a recent meta-analysis of the accuracy of MB alone in SLN mapping for breast cancer revealed an acceptable identification rate of 91% but unacceptable false negative rates (13%) according to standards recommended by the American Society of Breast Surgeons *(Li et al., 2018)*. Furthermore, a more extensive meta-analysis review of breast carcinoma and melanoma showed a SLN identification rate of 85% (breast carcinoma, range: 65-100%) and 84% (melanoma, range: 59-100%) using blue dye alone, while for radiocolloid alone it was 94% (range: 67-100%) and 99% (range: 83-100%), respectively. Using a combined method (radiocolloid and blue dye), the identification rates were 95% (breast carcinoma, range 94-95%) and 98% (melanoma, range: 98-98%) *(Niebling et al., 2016)*. These data favor the use of radiocolloid or combined technique for SLN mapping, specifying that the greatest utility of dyes is the visual guidance during surgery.

The use of combined techniques with blue dyes for SLN detection have been also described in veterinary medicine. Balogh and colleagues in 2002 were the first demonstrating that the principles of SLN detection hold in the field of canine oncology, describing SLN mapping with a combined technique in 24 client-owned dogs with spontaneous occurring tumors. Regarding blue dyes, they proved that only 77% of the SLN detected with radiocolloid were stained by the peritumorally injected patent blue solution. Ten years later *(2012)*, Worley described SLN mapping in 19 dogs with mast cell tumors (MCT) using radiocolloids combined with MB dye: of the 31 “hot” lymph nodes, just one was not visibly blue stained. In 2016, Brissot and Edery investigated the use of indirect lymphography with iodized oil combined with MB injection in dogs with different malignancies, observing only an 84.6% agreement between the two tracers. Grimes et al. *(2020)* described SLN mapping in 15 dogs with melanoma or MCT combining preoperative indirect computed-tomography (CT) lymphangiography with intraoperative MB peritumoral administration. The blue stained lymph nodes corresponded to the one identified on CT-lymphangiography in 18 out of 21 SLN (85,7%). No blue dye was observed in the remaining 3 lymph node and MB did not stain additional lymph nodes that had not been previously identified on CT-lymphangiography.

Besides systemic and local reactions and inconsistent identification rates, an additional disadvantage of this dyes is the peritumoral blue staining of the skin following the injection,

which can make intraoperative evaluation of tumor surgical margins challenging. Intraoperative SLN mapping using blue dye alone is a difficult technique, since deeply located stained lymphatics may be complicated to find and their dissection may require significant expertise *(Liptak et al., 2019)*. For these reasons, different vital dyes have been investigated for SLN mapping, such as autologous hemosiderin and fluorescent tracers. Pinheiro et al. *(2009)* described the use of hemosiderin from autologous blood combined with radiocolloid for mammary SLN identification in 6 experimental dogs. The technique was compared to patent blue dye and radiocolloid injected in the contralateral mammary gland of each dog. Autologous hemosiderin stained the SLNs brown and was as effective as patent blue dye for SLN identification. However, no further clinical studies on this tracer are available in veterinary medicine.

Near-infrared (NIR) imaging techniques rely on fluorescent tracers that absorbs NIR light (650-900 nm) and re-emits it at a lower energy. A NIR camera system detects the emitted light and converts it in a real-time video displayed on a screen, where the surgeon can visualize the fluorescent agent pathway. The most commonly used NIR fluorophore belongs to the cyanine dye class, in particular indocyanine green (ICG), which has the excitation peaks around 800 nm *(van Manen et al., 2018)*. The main limitation of this technique is its poor tissue penetration, up to few centimeters, so it is currently used for superficial imaging (such as transcutaneous SLN identification) or for image-guided surgery *(Kosaka et al., 2009)*. This method is evolving as one of the preferred intraoperative techniques in human patients with visceral tumors in the chest, abdomen or pelvis for *in vivo* cancer detection with both nonspecific fluorescent agents and cancer-targeted agents *(Uren et al., 2015)*. The intravenous administration of this dyes provides the visual identification of tumor's margins during surgery, allowing wide tumor resection with intraoperative assessment of residual neoplastic cells in the tumor bed. This innovative *in vivo* imaging system proved its potential in disease local control during clinical trials in dogs with spontaneous malignant tumors *(Cabon et al., 2016; Fidel et al., 2015; Eward et al., 2013; Reynolds et al., 1999)*.

Near-infrared fluorescence imaging has been proposed as an additional modality for intraoperative SLN mapping in abdominal malignancies (esophageal, gastric, colorectal, bladder, prostate, uterine, and ovarian cancer) *(van Manen et al., 2018)*, breast cancer and melanoma *(Niebling et al., 2016; Kosaka et al., 2009)*. Several validation studies have been conducted on animal models investigating preoperative SLN mapping and intraoperative navigation for visceral malignancies, such as the use of a fluorescent-labeled receptor-targeted radiopharmaceutical for prostate cancer *(Liss et al., 2014)* and the use of ICG in iodized oil emulsion for gastric tumor *(Kim et al., 2015)* in healthy beagle. Other NIR tracers have been validated in animal models, for example NIR fluorescent albumin and quantum dots for intraoperative SLN mapping in healthy dogs, pigs and in client-owned dogs with naturally occurring invasive transitional cell carcinoma of the urinary bladder *(Knapp et al., 2007)*.

Beyond intraoperative SLN mapping in patients with visceral tumors, NIR fluorescence imaging could be employed for transcutaneous detection of SLNs and the associated

lymphatics. Two recent studies proved the feasibility of ICG-based NIR fluorescence imaging for transcutaneous lymph nodes evaluation of the oral cavity *(Townsend et al., 2018)* and the axillary, inguinal and popliteal region *(Favril et al., 2019)* of healthy dogs, yet clinical trials on canine patients with spontaneous tumors are lacking. A recent abstract presented at 2019 ECVS Annual Scientific Meeting compared NIR imaging, lymphoscintigraphy and MB dye for intraoperative SLN mapping in 8 dogs with mast cell tumors *(Beer et al., 2019)*. Results showed a lower detection rate for ICG compared to radionuclides due to NIR reduced tissue penetration, which limited the detection to superficially located lymph nodes. Nevertheless, further studies are warranted to better characterized NIR fluorescence imaging potentiality for SLN mapping in tumor-bearing dogs.

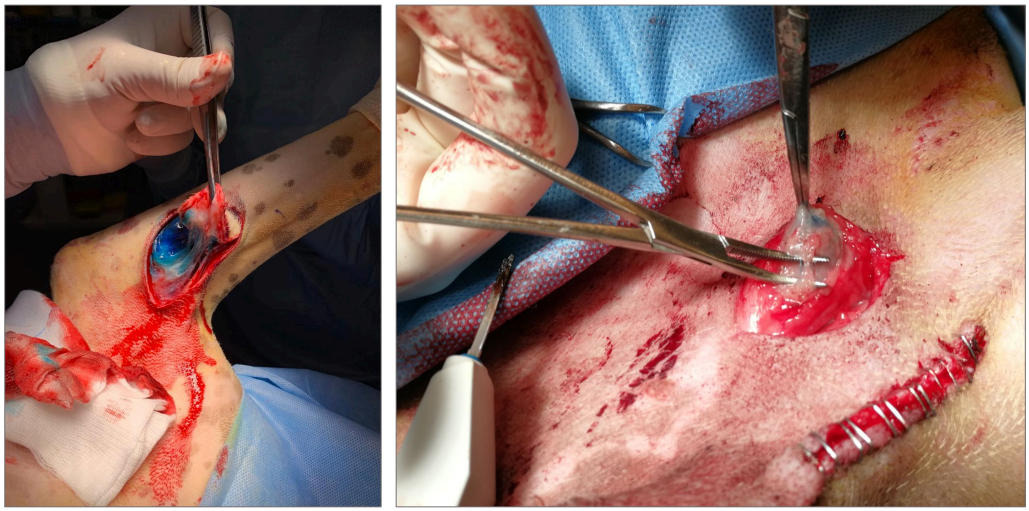

Figure 1.2 Intraoperative sentinel lymph node mapping with methylene blue guiding nodal extirpation in two dogs. *Courtesy of: Surgical oncology team, UNIMI Veterinary Teaching Hospital (Lodi)*.

1.3.2 Radiographic lymphography

For decades, radiographic lymphography has been considered the method of choice for imaging the lymphatic system. In fact, at the beginning of SLN research, Riveros and Cabanas *(1967)* performed lymphangiograms with iodized oil (*Lipiodol*) to identify tributary lymph nodes in cases of penile malignancies. Lymphography is performed after catheterization of a lymphatic vessel guided by a blue dye subcutaneous injection. The radiopaque contrast media is injected in the vessels at a very slow rate to avoid lymphatic rupture, then a set of radiograms of the region of interest is obtained *(Guermazi et al., 2003)*. An alternative technique is represented by indirect lymphography: the radiopaque contrast media is subcutaneously injected and indirectly drained by lymphatics. The contrast media historically employed for lymphography is Lipiodol, also known as ethiodized oil, an iodinated ethyl ester of the fatty acids of poppy seed oil, hydrophobic and water insoluble *(Kolbeck et al., 2011)*.

Conventional direct and indirect lymphangiography using Lipiodol have been investigated in experimental dogs for nodal radiation treatment field planning *(Mayer et al., 2013)*. In this study, direct lymphangiography resulted in uniform contrast uptake by an increased number of lymph nodes and fewer local side effects (3/16 injection sites) compared to the indirect technique (10/20 injection sites). Local side effects included swelling and erythema of the injection site at 14-28 days after the injection. One dog presented radiographic signs of pulmonary oil embolization 24h after the injection, a reported systemic side effects in human patients *(Guermazi et al., 2003)*, probably resulting from contrast venous intravasation. Despite these findings, indirect technique is preferred to direct lymphography for SLN mapping in oncological patient, since the former is supposed to accurately reflect the branching of the tumor lymphatic drainage.

Patsikas and Dessiris *(1996)* described the mammary glands lymphatic drainage pattern in 62 healthy mongrel bitches. Neither failing of the technique nor side effects were reported, though the lymphographic technique was not the objective of the study. The same research group repeated the study on 41 intact bitches bearing mammary tumors *(Patsikas et al., 2006)*, proving that the lymphatic drainage pattern in canine mammary tumors differs from normal glands, as stated by Pereira et al. *(2003)*. The authors also conducted an anatomical study on 73 clinically normal, lactating cats, describing the physiological mammary lymphatic patterns. For lymphatics identification they employed conventional radiology after intramammary Lipiodol injection in one group of cats (50) and both CT-indirect lymphography and plain radiography after iopamidol injection in a second group of animals (23). The results showed no differences in the mammary lymphatic drainage pattern between conventional and CT indirect lymphography *(Papadopoulou et al., 2009).* However, the authors did not comment the differences between the two employed contrast agents, even if indirect mammary lymphography using plain radiograms and water-soluble contrast media, such as iopamidol, has been reported as unsatisfactory due to the rapid absorption of the agent by blood vessels *(Pereira et al., 2003)*. The same research group published a further study more thoroughly investigating the potential of CT and radiographic indirect lymphography for mammary lymph node mapping in healthy cats. The authors firstly performed CT-indirect lymphography after intramammary injection of iopamidol, then after 24h each cat underwent intramammary injection of Lipiodol followed by a radiographic lymphography. The sentinel lymph node was not identified by both technique in 2/31 cats, while in the other cases the location of the SLN was the same for CT and radiographic indirect lymphography. In 3 cases, local signs of inflammation were reported after iodinized oil injection *(Patsikas et al., 2010)*.

In 2016, Brissot and Edery *(2016)* described the use of indirect lymphography with iodinized oil for SLN mapping in 29 dogs with 30 solid tumors. Indirect lymphography identified at least one draining node in all but one case, with a local complication only seen in one patient (blepharitis 10 days after the injection). The re-injection of contrast agent was necessary in 4 cases, in order to obtain sufficient nodal uptake. However, the mapping methodology used in this study was not standardized, alternating conventional radiography and computed

tomography as imaging techniques and using different contrast injection approaches, without direct comparisons.

A recent study compared lymphoscintigraphy and digital radiography for identification of SLN in 8 healthy experimental dogs *(Hlusko et al., 2020)*. The radiocolloid for lymphoscintigraphy and iohexol for indirect lymphography were injected into the subcutaneous tissues around a predefined area of skin on the brachium, 4 days apart one from the other. An SLN was identified in 8 dogs (100%) using lymphoscintigraphy and in 7 dogs (87.5%) using lymphography, but the identified SLN varied among dogs (either the axillary lymph node, the superficial cervical lymph node, or both) and techniques. The agreement between lymphoscintigraphy and lymphography studies was complete in 3/7 cases and partial in 4/7 cases, because 2/4 dogs had one SLN identified with lymphoscintigraphy and two SLNs with lymphography, and the other 2/4 dogs had two SLNs identified with lymphoscintigraphy and one with lymphography. This discrepancy could be attributed to efferent lymphatic drainage from the SLN to a second-tier node, as well as possible different injection site between the first and the second procedure. However, the differences in SLN detection based on the technique found in this study support the use of a combined SLN mapping protocol for oncological staging.

In veterinary practice, the use of radiographic lymphography for SLN mapping is cost-effective and technically simple to perform with accessible equipment. Nevertheless, the inconsistent identification rates and the reported sides effects – from swelling of the injection site to pulmonary oil embolization - should be taken into consideration.

1.3.3 CT - indirect lymphography

The technological advancement in cross-sectional imaging, with progressive widespread availability of computed tomography (CT), significantly curtailed the recourse to conventional lymphangiograms. In fact, CT imaging technique provides a more detailed anatomy and offers the possibility of three-dimensional reconstructions, avoiding radiographic superimposition.

Furthermore, CT-lymphography for SLN mapping became an appealing topic of research in human oncology due to socio-legal regulation and restrictions on radioisotope handling and disposal, and the costs of nuclear medicine equipment, especially for small centers or less developed countries. Therefore, preclinical studies have been conducted on animal experimental models, proving the possibility to apply this technique in veterinary oncological patients *(Lim et al., 2012; Suga et al., 2007; Hayashi et al., 2006; Suga et al., 2004; Suga et al., 2003[a]; Suga et al., 2003[b]; Wisner et al., 1994)*.

The contrast media most often used for CT-indirect lymphography is iopamidol, which is a nonionic, low-osmolar iodinated agent with a tested favorable safety profile and a good tolerance even when extravasated. This tracer is expected to migrate rapidly from the subcutaneous interstitial space to the lymphatics, similar to other water-soluble, low-molecular solutes. A similar compound used for SLN CT-lymphography is iohexol, which also belongs to second-generation nonionic contrast agent. Other specific tracers have been

investigated, such as lymphotropic iodinated nanoparticulates, but they showed slow penetration into the lymphatic system *(Suga et al., 2003[b]; Wisner et al., 1994)*.

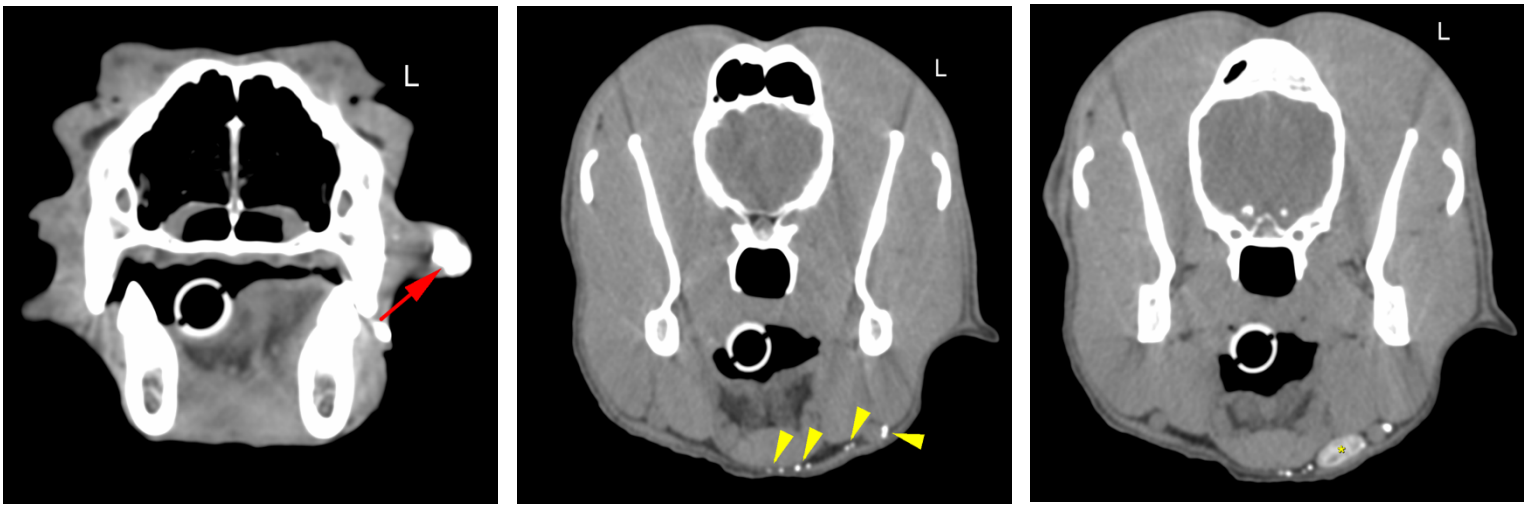

Figure 1.3 CT-indirect lymphography for sentinel lymph node mapping in a dog with oral melanoma. The contrast agent is peritumorally injected (red arrow) and drained by lymphatic vessels (yellow arrowheads), reaching the left mandibular node (*).

Over the past decade, several studies have been conducted on CT-indirect lymphography in dogs with different malignant diseases *(Rossi et al., 2018)*, including mammary tumors *(Soultani et al., 2016)* anal sac gland adenocarcinoma *(Majeski et al., 2017)*, head and neck malignancies *(Randall et al., 2020; Grimes et al., 2017)*, MCT, and melanoma *(Grimes et al., 2020)*. The reported SLN identification rates are different (60-100%), but all the researches show that CT- indirect lymphography is a feasible technique with minor injection-induced side effects (e.g., local inflammation, swelling, discomfort) and can be used for SLN mapping in dogs with different primary malignant tumors. Furthermore, in oncological patients this technique offers the possibility to combine lymphatic mapping with contrast enhanced-CT, which can provide valuable information for staging, tumor evaluation and surgical planning. In this case, intravenous contrast should be administrated prior to lymphangiography, because the bloom artifact generated from peritumoral injection of contrast agent may conceal the tumor site.

In 2016, Soultani and colleagues investigate the utility of CT-indirect lymphography in the assessment of SLN metastatic status in 33 dogs with mammary tumor, using criteria such as the lymph node morphology, the attenuation values and the opacification pattern. In human studies, partial lymph node staining or absence of lymph node opacification and stagnant lymphatic flow are reported as possible signs of lymph node metastasis *(Nakagawa et al., 2016)*. Soultani described 3 different enhancement patterns of the canine SLN: (1) homogeneous, characterized by uniform distribution of the contrast agent throughout the SLN parenchyma, (2) heterogeneous, with either patchy distribution of the contrast agent or

peripherical opacification of the SLN, (3) absence of SLN opacification. While the lymph nodes histologically negative for metastasis all demonstrated a homogeneous contrast uptake, the positive SLNs showed a heterogeneous enhancement in 13/16 cases, a homogeneous pattern in 1 case, and absence of opacification in 2 cases despite visible lymphatics connections. However, the hypothesis that nodal lymphographic CT appearance could be correlated to histopathological metastatic status was proved wrong four years later by Grimes et al. *(2020)* The authors performed a CT-indirect lymphography with subsequent MB-guided SLN extirpation in 15 dogs with diagnosed MCT (11) or melanoma (4). Eighteen SLNs were identified with both MB and CT-lymphangiography, while in 3 cases no MB dye was noted in the lymph node at the time of surgery. The SLN opacification pattern (heterogeneous, homogenous or peripheral) was not associated with the presence of metastasis, nor was the attenuation value at different times or the change in attenuation value. On the other hand, metastatic mechanical obstruction of lymphatic drainage and, therefore, absence of SLN opacification has been reported in others veterinary clinical studies *(Rossi et al., 2018; Majeski et al., 2017)*. Then again, clinical findings and information provided by staging contrast-enhanced CT, should allow the veterinary oncologist and radiologist to predict possibly involved lymph nodes by other criteria (i.e., markedly enlarged lymph nodes with heterogeneous enhancement).

CT-indirect lymphography has recently been compared to intraoperative radiocolloids detection and vital dye injection, to determine which technique more reliably identify the SLN in dogs with head and neck malignancies. Vital dye (MB or fluorescein) injection and radiocolloids identified the SLN in 17 of 18 and 20 of 20 dogs respectively, while CT-indirect lymphography showed draining lymphatic vessels in 18 of 20 dogs and identified the sentinel lymph node in 11 of 20 dogs *(Randall et al., 2020)*. In cases where lymphography fails to identify the lymph node, either contrast re-injection or massage and evaluation of the area of interest for possible restriction of lymphatic flow is warranted. In fact, attention needs to be paid to endotracheal tube ties and patient positioning to avoid possible obstruction of the lymphatic flow *(Grimes et al., 2017)*.

While a valuable advantage of CT-indirect lymphography is the possibility to visualize the anatomical details surrounding the identified SLN, other techniques are needed to be combined for intraoperative SLN detection. The correlation between CT findings and surgical operation field, as well as surgical localization of the SLN, may prove to be challenging. In fact, in human medicine CT-lymphography has not replaced the intraoperative use of vital dyes or radiocolloids for SLN mapping in oncological patients.

1.3.4 Contrast-enhanced ultrasound lymphosonography

Contrast-enhanced ultrasound (CEUS) is a safe, cost-effective, minimally invasive technique mainly used to increase the intensity of the blood pool echo signal *(Haers et al., 2009)*. It also proved to be effective in SLN detection both in human *(Moody et al., 2017)* and veterinary studies *(Fournier et al., 2020; Favril et al., 2019; Gelb et al., 2010; Wang et al., 2010; Lurie et*

al., 2006). The sonographic contrast agents (e.g., SonoVue®, Definity®) consist of microbubbles with a high-molecular weight gaseous core enclosed by a shell of lipids. After peritumoral injection, the lipophilic tracer is rapidly drained by lymphatics, reaching the SLN. The microbubbles strongly vibrate at the frequencies used for diagnostic ultrasound imaging, becoming several times more reflective than normal body tissues using both grey-scale or Doppler imaging.

Feasibility studies have been conducted in healthy dogs comparing lymphosonography to blue dye *(Wang et al., 2010)* and NIR fluorescence imaging *(Favril et al., 2019)*, and in canine patients with spontaneous head and neck tumors comparing CEUS to lymphoscintigraphy *(Lurie et al., 2006)*. The SLN detection rate of lymphosonography was 91.3% (21/23) *(Wang et al., 2010)* compared with blue dye and 100% compared to NIR imaging. In the clinical study on head and neck malignancies, lymphosonography identified the SLN in 8 out of 10 dogs (80%) and each lymph node identified by CEUS was also detected by lymphoscintigraphy. An additional recent study evaluated the safety and effectiveness of CEUS lymphosonography to detect SLNs in a larger cohort of dogs with mast cell tumors. CEUS identified at least one SLN in 59 out of 62 MCTs (95.2%), and no side effects related to tracer injection were reported *(Fournier et al., 2020)*.

As for CT-indirect lymphography, other techniques are needed to be combined with CEUS lymphosonography for intraoperative SLN detection. Another possible CEUS limitation lies in the operator-dependent search of the lymphatic basin containing the enhanced SLN. In a clinical setting, the operator would not previously know the patient lymphatic anatomy and would have to survey a relatively large tissue volume to unambiguously localize the SLN.

These studies suggest that CEUS lymphosonography is a safe and feasible adjunct to conventional techniques for SLN detection and US-guided minimally invasive lymph node biopsy. Furthermore, CEUS technique could also contribute to the assessment of lymph node metastatic status. In dogs with head and neck tumors, the presence of a filling defect in the mandibular lymph nodes after lymphosonography associated with a high-grade strain elastographic pattern were correlated with the presence of metastasis *(Choi et al., 2020)*. However, these findings need to be considered with caution, because even if CEUS enhancement patterns were significantly associated with the metastatic status of the SLN in dogs with MCT, lymphosonography only had a moderate agreement with histology *(Fournier et al., 2020)*.

1.3.5 Magnetic resonance

High field magnetic resonance provides detailed anatomical soft tissue imaging, with a high spatial resolution. Because of its proved utility in oncological staging, magnetic resonance imaging (MRI) has been under investigation both for SLN mapping using a lymphography technique and for the diagnosis of nodal metastasis using lymphotropic nanoparticles.

Like CT-indirect lymphography, MRI-indirect lymphography consists of peritumoral injection of a magnetic or paramagnetic contrast agent, which is drained by lymphatic vessel and

carried to the SLN. There are few experimental studies describing MRI-indirect lymphography with paramagnetic contrast agent (e.g., *gadopentetate dimeglumine*, *gadoversetamide*) as a feasible technique for mammary and head and neck SLN identification in healthy dogs *(Mayer et al., 2012; Suga et al., 2003[c])*. Specific MRI lymphotropic contrast agents have been developed and studied in animal experimental models for MRI-indirect lymphography - such as *gadofluorine 8*, a lipophilic but water-soluble gadolinium complex *(Misselwitz et al., 1999)*, and *gadofosveset trisodium*, an albumin-binding small molecule gadolinium chelate *(Turkbey et al., 2015)* -, and for the detection of nodal metastasis in oncological staging, - such as ultra-small paramagnetic iron oxide particles (USPIO). These iron nanoparticles are phagocytized by macrophages in normal lymph nodes, resulting in regions of drastic signal to noise ratio decrease secondary to a susceptibility artefact on gradient echo MRI sequences. The presence of nodal metastasis determines a substantial decrease in the number of macrophages and therefore decrease of voiding artefacts after intravenous USPIO administration. A recent pilot study on 6 dogs with various oral tumors shows that lymphotropic nanoparticle enhanced MRI using intravenous injection of *ferumoxytol* (i.e., a second-generation USPIO compound) has the potential to be a sensitive and specific method to detect lymph node metastasis *(Griffin et al., 2019)*. Further studies with a larger sample size are required to assess the clinical utility of MRI in SLN mapping and nodal metastasis diagnosis in veterinary oncological patients.

1.3.6 Lymphoscintigraphy

The most widely used technique for SLN mapping is the combined method with peritumoral injection of blue dye and technetium-99m(^{99m}Tc)-labelled nanocolloid. Radioactive tracers (i.e., radiocolloids) emit gamma rays, which are picked up by a gamma camera and can be used for both preoperative planar lymphoscintigraphy, obtaining planar images of the radiopharmaceutical distribution, as well as intraoperative nodal detection with a hand-held gamma probe *(Figure 1.4)*, which guide the surgeon towards the SLN even if locate in deep tissue layers.

The most commonly employed radionuclide is ^{99m}Tc, a metastable nuclear isomer of technetium-99 which emits gamma (photons) rays between 140.5 keV (98.6%) and 142.6 keV (1.4%) and has a relatively short physical half-life (6.01 hours), which allows the reduction of patient total radiation exposure *(Keshtgar et al., 1999)*. However, the short half-life precludes the possibility of radionuclide storage and complicate the transport. Therefore, ^{99m}Tc is obtained directly in the user facility from a generator extracting the isotope from the parent nuclide, molybdenum-99, which has a longer half-life (66 hours). The radionuclides separation is usually achieved by column chromatography, using saline solutions to elute ^{99m}Tc from molybdate *(Van et al., 2014)*. This process can be repeated for up to two weeks, by which time the molybdenum-99 activity will be about 3% of its original value.

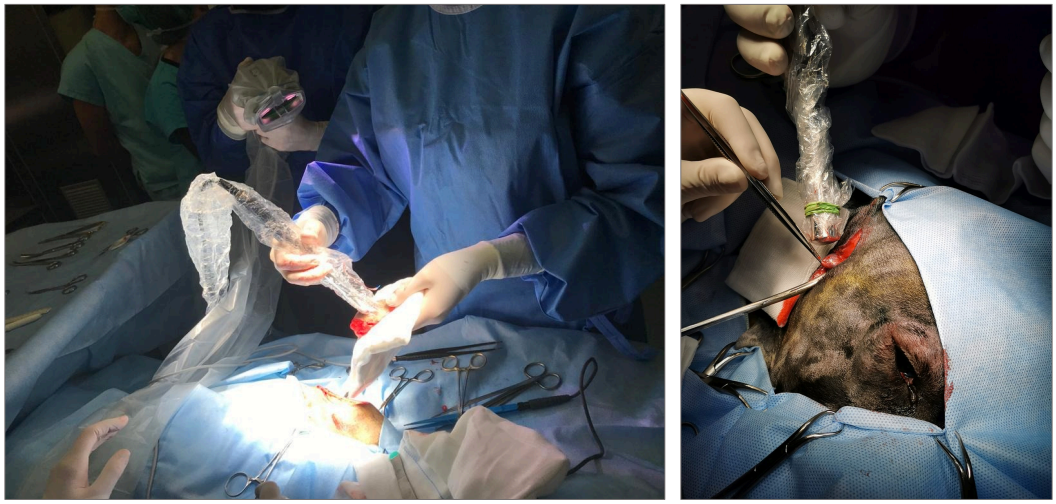

Figure 1.4 Intraoperative sentinel lymph node mapping with handheld gamma probe guiding nodal extirpation in two dogs. *Courtesy of: Surgical oncology team, UNIMI Veterinary Teaching Hospital (Lodi)*.

The colloids used to label ^{99m}Tc for SLN detection includes the sulfur colloid (<200 nm), human serum albumin nanoparticles (<80 nm), and antimony sulfide colloid (10 nm).
The colloid particles size and the surface characteristics affect both the radiotracer drainage rate from the injection site to the peritumoral lymphatic vessel as well as the phagocytotic uptake by macrophages and tissue histiocytes that line the subcapsular sinus of lymph nodes. From the extracellular matrix, particles are transported by both convection and diffusion, in particular small molecules are mostly transported by diffusion, which is a slow process over longer distances; instead, larger molecules maintain mechanical interactions with the extracellular components, which slows down the particle movements *(Erba et al., 2013)*. Therefore, larger colloid particles (> 500 nm) can be indefinitely retained at the injection site, whereas the smallest particles (<5 nm) are rapidly cleared penetrating lymphatic and blood capillaries *(IAEA, 2009)*. Although tracers with smaller particle size (<50 nm) ensure visualization of a greater number of LNs, they lead to difficulties in image interpretation and intraoperative SLN identification *(Keshtgar et al., 1999)*. While one part of the colloid lasts inside the lymph node, phagocytized by macrophages and histiocytes, the smaller-size remaining fraction proceeds through the efferent lymph vessels toward the second echelon nodes, which could challenge intraoperative radio-guided SLN detection *(Erba et al., 2013)*.
Filtered sulfur colloid is a widely used and effective tracer but is minimally absorbed (<5%) from the injection site, requiring prolonged imaging times. Besides, in order to retain its stability, ^{99m}Tc-sulfur colloid has acidic pH, which often causes burning pain at the injection site. On the other hand, human serum albumin nanocolloid has a reduced incidence of side effects, and the radiopharmaceutical preparation is also simpler compared to other colloids. The albumin particles size biodistribution is standardized (95% of the particles are ≤80 nm), allowing a rapid clearance from the injection site *(Erba et al., 2013)*.

Figure 1.5 The SPECT gantry with a single head gamma camera used in the UNIMI Veterinary Teaching Hospital, (Lodi).

Only a few studies have described the use of radiocolloids for SLN detection in veterinary patients with spontaneous tumors *(Balogh et al., 2002; Lurie et al., 2006; Worley et al., 2012; Randall et al., 2020; Linden et al., 2019; Ferrari et al., 2020)*, likely due to the restrictive access to radionuclides and the high cost of the equipment. Nevertheless, lymphoscintigraphy is still the gold standard in human oncology *(Inubushi et al., 2018)* for SLN mapping in patients affected by cutaneous melanoma *(Tardelli et al., 2016)* and breast cancer *(Manca et al., 2016)*. As previously mentioned, in 2002 Balogh and colleagues introduced the SLN concept in veterinary oncology conducting a pilot study on 24 client-owned dogs with spontaneously occurring tumors (mammary neoplasia, fibrosarcoma, thyroid and parathyroid carcinoma) using ^{99m}Tc-human serum albumin and Patent blue injection. The authors identified a total of 35 SLN, of which 34 found by radioguided surgery (97%), 31 by planar lymphoscintigraphy (88%) and 27 by blue dye injection (77%). It appears odd that all the 35 identified SLN are reported to be metastatic, even in a dog with mammary adenoma. Nevertheless, the study demonstrated that combined SLN mapping with planar lymphoscintigraphy, intraoperative radioguided surgery and blue dye is a sensitive and safe technique in canine oncological patients.

The impact of SLN mapping on canine oncological staging have been investigated by Worley in 2012. In this study, ^{99m}Tc-sulphur colloid was used for planar lymphoscintigraphy and radioguided surgery combined with blue dye injection in 19 dogs with MCTs. The SLN mapping procedure allowed a more accurate oncological staging, offering to 8 dogs an additional adjuvant therapy that would otherwise been excluded. Our research group have recently

published a study supporting the importance of SLN mapping and extirpation for a personalized staging approach in dogs with MCT (*Ferrari, 2020*).

Feasibility studies in healthy dogs have been performed investigating radiocolloids for lymph node mapping of mammary glands, anal sacs, and lungs. In particular, Pereira and colleagues *(2008)* proved the feasibility of mammary lymph node detection trough planar lymphoscintigraphy in healthy bitches. Their work offers an accurate technical protocol with intramammary administration of ^{99m}Tc-labeled dextran, a polysaccharide (70,000 Da) used for functional lymphatic studies. A reported limitation of lymphoscintigraphy is the lack of anatomical details and referencing points, but this can be solved using a radioactive source, such as the syringe with residual radiopharmaceutical, as a guiding pointer *(Pereira, 2008)*. Linden et al. *(2019)* conducted a prospective pilot study to establish the feasibility of lymphoscintigraphy using ^{99m}Tc-sulphur colloid for the anal sac of 8 healthy Beagle dogs, comparing intramural and perimural injection techniques. Based on the results, lymphoscintigraphy of the anal sac proved to be a feasible and safe procedure and the intramural injection technique was deemed superior in five dogs (62.5%). Two different studies investigated intraoperative pulmonary lymph node mapping with blue dye (isosulfan blue and MB) and ^{99m}Tc-sulphur colloid lobar injection in healthy dogs. In both studies, thoracic lymph node localization proved to be challenging and the results showed that further investigation for pulmonary SLN detection are mandatory *(Nwogu et al., 2002; Tuohy & Worley 2014)*.

Radiocolloids have been used as the reference standard to validate other SLN mapping technique, such as CEUS *(Lurie et al., 2006)* and CT-indirect lymphography *(Randall et al., 2020)*. In both studies, lymphoscintigraphy and radio-guided surgery were the more reliable sentinel lymph node technique, with the higher detection rate.

Besides lymphoscintigraphy and radioguided surgery, radiocolloids can be employed for single-photon emission computed tomography (SPECT). In particular, SPECT/CT combines the higher detection rate of scintigraphy with the increased anatomical details of CT, allowing a more accurate anatomical mapping of the lymphatic system *(Naaman et al., 2016)*. There is no available literature on SPECT/CT for SLN detection in veterinary oncology, due to the limited availability of the required equipment.

2. Preoperative planar lymphoscintigraphy for sentinel lymph node mapping in 51 dogs and one cat with spontaneous malignant tumors

Abstract presented at the European College of Veterinary Diagnostic Imaging Online Congress; September 17-18, 2020.
Study submitted to Veterinary Radiology & Ultrasound: under revision.

Abstract

Sentinel lymph node (SLN) mapping is the current gold standard for the oncological staging of solid malignancies in humans. This study describes the feasibility of preoperative lymphoscintigraphy for SLN detection in canines and a feline with spontaneous malignancies and the improvements in staging accuracy. Client-owned dogs and cats with confirmed malignant neoplasia, absence of distant metastasis, and absence of regional lymphadenomegaly were prospectively enrolled in this observational study. Lymphoscintigraphy was performed after the peritumoral injection of Technetium-99m labeled nanocolloids. Regional dynamic and static images were acquired, with and without masking of the injection site with a lead shield. The dogs were then subjected to surgery for tumor excision and SLN extirpation. Intraoperative SLN detection was performed by combining methylene blue dye and a dedicated gamma probe. Overall, 51 dogs and 1 cat with a total of 60 solid malignant tumors were enrolled. Lymphoscintigraphy identified at least one SLN in 57/60 cases (95%). The SLN did not always correspond to the regional lymph node (35/57, 61.4%). The use of a lead shield, masking the injection site, markedly improved the SLN visualization. The median time of SLN appearance was 11.4±9.3 min. No side effects were observed. Preoperative lymphoscintigraphy allows for SLN detection in dogs and cats and can improve staging accuracy by either identifying the SLN in a different lymphosome than clinically expected or discriminating the draining node in uncertain cases. The combined use of preoperative and intraoperative techniques is recommended to increase the SLN detection rate.

2.1 Aim of the study

The present study aimed to describe the feasibility, safety, and efficacy of preoperative lymphoscintigraphy for SLN detection in canine and feline patients with spontaneous malignancies in different anatomical locations. We further investigated whether the first LN draining the tumor site could be identified within unexpected lymphatic basins compared to anatomic RLNs.

We hypothesize the following: 1. Peritumoral injection of 99m-Tc-labeled nanosized human serum albumin allows rapid detection of SLN and the associated lymphatic pathway; 2. The first LN draining the tumor site can be identified within unexpected lymphatic basins compared to anatomic RLNs.

2.2 Materials and methods

Patients

Client-owned dogs and cats admitted to a veterinary institution for oncological surgery were prospectively enrolled in this observational study. The inclusion criteria were as follows: 1. Cytological or histologically confirmed spontaneous malignant neoplasia (first presentation or recurrence), 2. Tumors amenable for surgical excision and accessible for peritumoral injection; 3. No-palpable or clinically unaltered (symmetrically palpable in the contralateral lymphatic basin) RLNs, and 4. Absence of distant metastasis at admission, according to the staging reference guidelines for each tumor. All the procedures were conducted following the European legislation concerning Animal Protection and Welfare (Directive 2010/63/EU) and the Italian ethical law (Decreto Legislativo 04/03/2014, n.26). A client-signed informed consent was obtained for each procedure. Since the data used in this study were collected as part of a routine clinical activity, no ethical committee approval was required. Each animal received appropriate tumor staging, blood testing, and presurgical workup according to the type of neoplasia, comorbidities, and/or presenting clinical signs.

Planar lymphoscintigraphy

Lymphoscintigraphy was performed with animals under general anesthesia. A ^{99m}-Tc labeled nanosized human serum albumin (NANOALBUMON, Radiopharmacy Laboratory Ltd., Budaörs, Hungary) solution was prepared using 0.9% NaCl as a solvent. Each patient received 10-35 MBq/0.5 ml, injected using a 25-G needle subcutaneously in 4 quadrants around the primary tumor. The MBq dose of the syringe was measured using a dose calibrator (ATOMLAB 100Plus, Biodex Medical Systems, Shirley, New York), before and after the injection to calculate the administered dose *(Balogh et al., 2002)*.

Regional dynamic images (ventral view, 1 frame/s for 60 s, matrix size 256x256) were captured immediately after the injection (T0), then after 3 (T1) and 8 (T2) min with a single

head gamma camera (Picker Prism 1000XP, Picker International, Highland Heights, Ohio). If needed, the injection site (IS) was masked with a 2 mm thick lead shield of appropriate size. Two ventral or dorsal images and two lateral static images (*Figures 2.1A-B*), centered on the tumor site, were acquired (120 s/frame, matrix size 256x256) immediately after the dynamic study. Each lateral (left or right) and ventral or dorsal views were selected based on the minor distance between the tumor and the gamma camera to improve the lymphatic uptake visualization (*Figure 2.1B*). For one image per positioning, the IS was masked with a lead shield. If required, additional images were taken by centering the gamma camera cranially/caudally to the region of interest or by changing the patient's positioning until the first draining LN was identified.

Looking at the real-time images of the gamma camera persistence oscilloscope (P-scope), the syringe with residual dose was used as a pointer to identify the SLN based on the syringe position relative to the patient's anatomical structures *(Balogh et al., 2002; Pereira et al., 2008)*. In patients with more than one primary tumor, the injection and image acquisition were performed separately for each tumor in the same session.

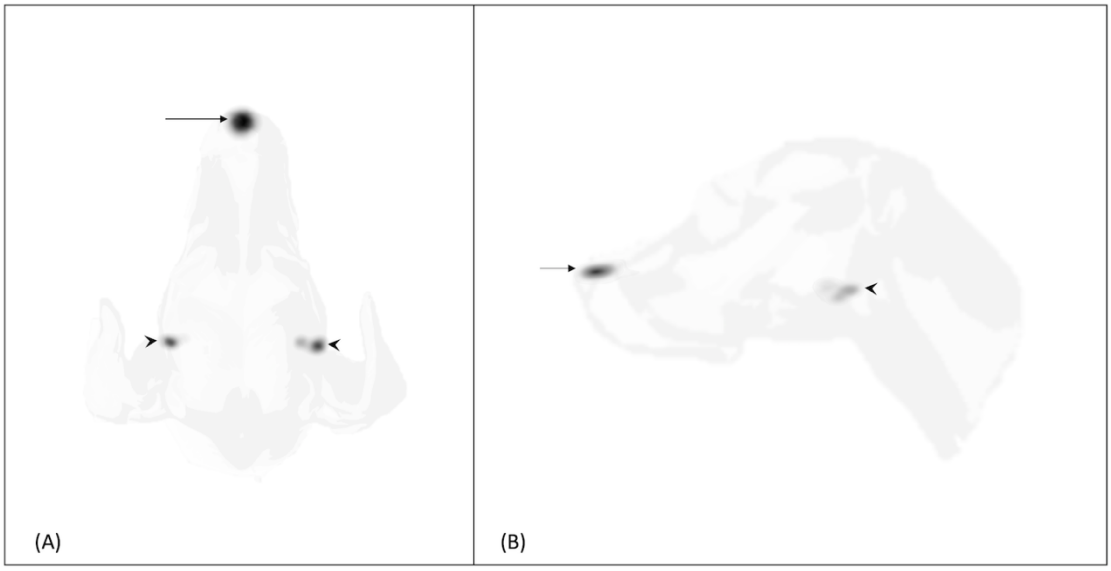

FIGURE 2.1 Dorsal (A) and right lateral (B) planar static images of the head of a dog with a single MCT at the planum nasale, acquired 3 minutes after injection. Injection site (arrow) was not masked, and a bilateral radiopharmaceutical uptake was observed at the level of mandibular LNs (arrowheads).

Intraoperative SLN detection

After lymphoscintigraphy, the animals were admitted to surgery for tumor excision and SLN extirpation *lege artis*. Prior to the surgical site's aseptic preparation, 0.4 ml of 5 mg/ml sterile MB (S.A.L.F. S.p.A, Cenate Sotto, Bergamo, Italy) was peritumorally injected in the radiopharmaceutical inoculation sites *(Balogh et al., 2002; Worley et al., 2012; Randall et al., 2020; Ferrari et al., 2020)*. The audible sounds and counts visible on the gamma probe console (Crystal probe SG04, Crystal Photonic GmbH, Berlin, Germany), alongside MB visualization, guided the surgical dissection during the lymphadenectomy procedure. Any LN presenting a blue stain or a radioactive count (RC) at least twice the RC of a distant body region (background counts), was extirpated. The surgeon then checked the operation site with the gamma probe and evaluated the residual radioactivity. Any other LN with an RC equal to or greater than 10% of the LN with the highest RC, was removed *(Worley et al., 2012; Ferrari et al., 2020)*. Primary tumor and extirpated LN were checked *ex vivo* with the detector and then fixed in 10% neutral-buffered formalin for a routine histopathological examination *(Weishaar et al., 2014)*. Animals were hospitalized for at least 24 h after surgery.

Data analysis

Descriptive analysis was performed on the following data: patient signalment, tumor type, presentation (first vs. recurrence), and the localization based on the lymphatic territories identified by Suami et al. *(2013, Figure 2.2).* Sentinel lymph nodes detected with lymphoscintigraphy, gamma probe, and MB were recorded and compared to the RLNs reported to normally drain the tumor's anatomical territory. Other recorded data included the presence or absence of histopathologic LN metastasis, radiotracer, and MB side effects.

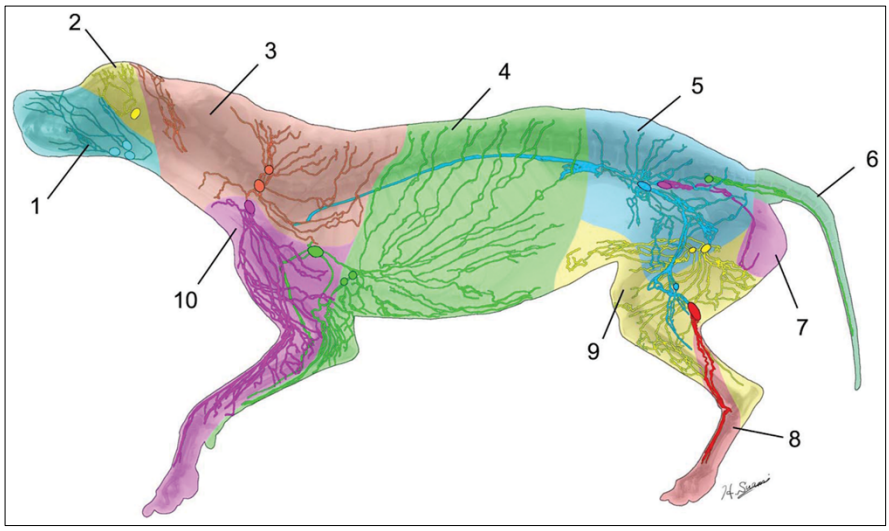

FIGURE 2.2 Color-coded diagram of the lymphatic territories (lymphosomes): 1, submandibular; 2, parotid; 3, dorsal superficial cervical; 4, axillary; 5, medial iliac; 6, lateral sacral; 7, hypogastric; 8, popliteal; 9, superficial inguinal; and 10, ventral superficial cervical. Figure previously published in PLoS One. 2013;8(7): e69222. *https://doi.org/10.1371/journal.pone.006922*

2.3 Results

Patients

Fifty-one dogs and one cat were enrolled in the study. The ages of dogs ranged from 1 to 15 years (mean, 7.9 ±3.2 years; mode, 10 years; median, 8 years); weights ranged from 3.2 to 51 kg (mean, 26.8 ±12.4). Twenty-eight of the dogs were male (10 neutered) and 23 were female (20 spayed). There were 12 mixed breed dogs; 9 Labrador retrievers; 6 Golden retrievers; 3 Dogo Argentinos; 2 Boxers; 2 American Staffordshire Terriers; 2 English setters, and one each of other 15 breeds. The total number of tumors investigated in the dogs were 59, including mast cell tumor (MCT, n=47), mammary adenocarcinoma (n=3), oral melanoma (n=2), thyroid carcinoma (n=2), cutaneous squamous cell carcinoma (SCC, n=1), parotid adenocarcinoma (n=1), perivascular wall tumor (myopericytoma, n=1), oral undifferentiated sarcoma (n=1), and benign mixed mammary tumor (n=1). The inclusion of benign mammary neoplasia was due to an initial diagnosis of a malignant tumor on the cytological examination. The patient presented again after 2 months for an SLN mapping of adenocarcinoma on the contralateral mammary row. Another dog with multiple cutaneous MCTs, presented after 2 years for MCT at a different anatomical site. Six dogs had more than one primary tumor: two presented with 3 cutaneous MCTs (*n = 6*, *31*), three had 2 cutaneous MCTs (*n = 10*, *13*, *and 17*), and one had 2 mammary adenocarcinomas (*n = 41*). Two dogs presented with MCT recurrences; in particular patient no. 3 underwent surgery with a right prescapular lymphadenectomy and

adjuvant radiation therapy. The distribution of lymphatic territory based on the tumor site is shown in *Table 2.2*.
The only feline patient included in the study was a 13-years-old neutered female domestic short-haired cat with recurrence of a mandibular symphysis SCC.

Sentinel lymph node detection

Lymphoscintigraphy located the SLN in 57 of the 60 tumors (95%). Dynamic images allowed SLN identification in 15/57 cases (T0 in 14 cases, T2 in 1 case), whereas only a lymphatic radiotracer pathway was visible in the other 23 procedures.
Subsequent static images detected SLN in all 57 cases; in 22/57 tumors, the SLN was observed on the first static image (9/10 min after injection). The median time of SLN appearance on planar images was 11.4 ±9.3 min (range: 9-42 min).
The radiotracer failed to identify the SLN in three cases. In the first dog with palpable thyroid carcinoma, a local radiotracer diffusion was observed after the peritumoral injection, but neither draining node nor lymphatic pathways were detected. Similarly, for patient no. 3, which presented an MCT recurrence after surgical excision, only a subcutaneous radiotracer diffusion was observed without SLN identification. In the other dog with a thyroid tumor, an ultrasound-guided intratumoral radiotracer injection was performed[24], but no radiocolloid migration was observed.
The LNs identified with lymphoscintigraphy corresponded to RLN in 22 of the 57 cases (38.6%). In 10 of the 22 matching cases, lymphoscintigraphy allowed for SLN identification within the axillary lymphatic territory among the axillary LN, accessory axillary LN, or both. In 18 cases (31,6%), the tumor anatomical site was borderline between two different lymphosomes and lymphoscintigraphy allowed the discrimination of the draining SLN. In 8 cases (14%), lymphoscintigraphy detected a second SLN in a different lymphatic territory from the tumor lymphosome. In 9 cases (15,8%), the identified SLNs did not correspond to the RLN.
The gamma probe intraoperatively confirmed the SLN detected using lymphoscintigraphy in all the cases. In two patients (n = 16, 18) with an MCT of the right stifle, the gamma probe identified an additional radioactive LN in the popliteal basin, which was not recognized by lymphoscintigraphy. Methylene blue injection was used in 51 cases and identified the draining LNs in 46 (90.2%). Blue-stained LNs corresponded to radioactive LNs in 45 cases. In a dog with sub-lingual SCC (n = 33), MB identified an additional metastatic LN in the contralateral mandibular basin. In patient number 3, where the radiotracer failed to identify the SLN, the MB migrated to the LN draining the MCT recurrence site. In one case (n = 44) with a sternal MCT, MB stained the left prescapular LN but not the contralateral radioactive LN; both were confirmed as early metastatic on the histopathological examination ($HN2^6$). In 4 cases, the MB did not stain any LN.
Patient no. 22 (MCT of the right stifle) showed a radiotracer and MB uptake of a right inguinal structure, that was histologically identified as focal inflammatory infiltration of connective tissue composed by mast cells and eosinophils. This patient had previously undergone an ipsilateral unilateral mastectomy for a mammary tumor.

Lymphadenectomy was performed in 53/60 tumors. As for the MCT cases, histopathological classification *(Weishaar, 2014)* revealed absence of metastasis (HN0) in 15/44 cases, pre-metastatic nodal lesion (HN1) in 7/44 cases, early metastasis (HN2) in 18/44 cases, and overt metastasis (HN3) in 4/44 cases. As for the other malignancies, 2/9 patients presented metastasis on the histopathological examination (n = 33, SCC; n = 38, oral melanoma).

Table 2.1 Signalment (breed, sex, age, weight) and neoplasia of the 51 dogs and 1 cat included in the study.
Abbreviations: Pt, patient; M, male; F, female; n, neutered; MCT, mast cell tumor; SCC, squamous cell carcinoma.

PT	BREED	SEX	AGE	WEIGHT(KG)	NEOPLASIA
1	Beagle	M	13	16	MCT
2	Mixed breed	Fn	6	18	MCT
3	Mixed breed	Fn	11	7.3	MCT - recurrence
4	Golden Retriever	M	3.5	37	MCT
5	Bracco Italiano	M	3.5	31	MCT
6	Dogo Argentino	M	6	41.5	MCT
7	Labrador	Fn	8	31	MCT
8	Amstaff	M	5	34	MCT
9	Labrador	M	6	27	MCT
10	Dogo Argentino	M	10	51	MCT
11	Labrador	M	10	33	MCT
12	Golden Retriever	Fn	7	33	MCT
13	Mixed breed	Fn	14	33	MCT
14	Swiss Mountain Dog	F	4	34	MCT
15	Labrador	Mn	9	34	MCT
16	Boxer	M	8	38	MCT
17	Pug	M	3.5	9.7	MCT
18	Golden Retriever	Fn	7.5	31	MCT - recurrence
19	Weimaraner	Mn	7	35	MCT
20	Labrador	Fn	6	31	MCT
21	Labrador	M	1	32	MCT
22	Yorkshire Terrier	Fn	13	5	MCT
23	Golden Retriever	Fn	11	26	MCT
24	Dachshund	Fn	9	5.7	MCT
25	Labrador	M	7	35	MCT
26	Maltese	Fn	7	3.5	MCT
27	Golden Retriever	Mn	12	37	Melanoma
28	English Setter	M	7	20	MCT
29	Mixed breed	Mn	10	47	Parotid Adenocarcinoma
30	Mixed breed	Mn	4	23	MCT
31	Mixed breed	Mn	12	22	MCT
32	Mixed breed	Fn	10	23	Thyroid Carcinoma
33	Pinscher	M	15	6.4	SCC
34	Chihuahua	Mn	9	3.2	MCT
35	Mixed breed	Fn	7	11	Benign Mammary Tumor
36	Segugio Italiano	M	9	19.4	Thyroid Carcinoma
37	Boxer	M	9	42	MCT
38	Rhodesian Ridgeback	Mn	8	45.8	Melanoma
39	Mixed breed	F	10	31	Mammary Carcinoma
40	Chow Cow	Fn	1	20.7	Sarcoma
41	Mixed breed	Fn	8	11	Mammary Carcinoma
42	English Setter	Fn	10	15	MCT
43	Mixed breed	Fn	10	18	PWT
44	Labrador	F	4	27.6	MCT
45	Mixed breed	Fn	11	36.5	MCT
46	Golden Retriever	Fn	6	27.2	MCT
47	Amstaff	Mn	4	35	MCT
48	Labrador	Mn	8	41	MCT
49	Cocker Spaniel	Fn	8	12	MCT
50	Dogo Argentino	M	10	42	MCT
51	Pitbull	M	3	35.5	MCT
52	Domestic Short Air	Fn	13	5	SCC - recurrence

Table 2.2 Tumor sites, corresponding lymphosomes, and SLN detected with lymphoscintigraphy and intraoperative techniques in 51 dogs and 1 cat (n. 52). In three patients (n. 10, 18, 43), the intraoperative SLN detection was not performed since the owner refused lymphadenectomy. Methylene blue injection was not performed in 4 patients (n. 29, 31, 32, 51) and intraoperative gamma probe detection was not possible in 2 cases (n. 44, 46) due to probe malfunctioning.

Abbreviations: Pt, patient; MB, methylene blue; MCT, mast cell tumor; SCC, squamous cell carcinoma; R, right; L, left; LNA, lymphadenectomy; NP, not performed. *Histopathology identified inflammatory infiltration of connective tissue composed by mast cells and eosinophils.

PT	TUMOR	TUMOR SITE	LYMPHOSOME	LYMPHOSCINTIGRAPHY	GAMMA PROBE	MB DYE
1	MCT	R caudo-ventral neck	R ventral cervical	R prescapular	R prescapular	R prescapular
2	MCT	R ischiatic region	R hypogastric R inguinal	R inguinal	R inguinal	R inguinal
3	MCT - recurrence	R shoulder	R dorsal cervical R axillary	none	none	R accessory axillary
4	MCT	L thorax (XIII rib)	L axillary	L accessory axillary	L accessory axillary	L accessory axillary
5	MCT	L thorax (XIII rib)	L axillary	L accessory axillary	L accessory axillary	L accessory axillary
6A	MCT	R stifle	R inguinal	R inguinal	R inguinal	R inguinal
6B	MCT	L stifle fold	L inguinal L medial iliac	L inguinal	L inguinal	L inguinal
6C	MCT	sternum - R lateral	R axillary	R prescapular	R prescapular	R prescapular
7	MCT	R stifle	R inguinal	R popliteal R inguinal	R popliteal R inguinal	R popliteal R inguinal
8	MCT	L preputial	L inguinal	L inguinal	L inguinal	L inguinal
9	MCT	R stifle	R inguinal	R popliteal R inguinal	R popliteal R inguinal	R popliteal R inguinal
10	MCT	thorax - R caudodorsal	R axillary	R axillary	no LNA	no LNA
10A	MCT	thorax - L cranioventral	L axillary	L axillary	no LNA	no LNA
11	MCT	scrotum	R/L inguinal	R inguinal	R inguinal	R inguinal
12	MCT	L shoulder	L dorsal cervica L ventral cervical	L prescapular	L prescapular	L prescapular
13A	MCT	III-IV L mammary gland	L axillary L inguinal	L inguinal	L inguinal	L inguinal
13B	MCT	III digit R foot	R popliteal	R popliteal	R popliteal	R popliteal
14	MCT	R forearm	R ventral cervical R axillary	R axillary R prescapular	R axillary R prescapular	R axillary R prescapular
15	MCT	thorax - R lateral	R axillary	R axillary	R axillary	R axillary
16	MCT	R stifle	R inguinal	R inguinal	R inguinal R popliteal	R inguinal R popliteal
17A	MCT	L ear base	L dorsal cervical L parotid	L prescapular	L prescapular	L prescapular
17B	MCT	R suprascapolar region	R dorsal cervical	R prescapular	R prescapular	R prescapular
18	MCT - recurrence	L stifle fold	L inguinal L medial iliac	L medial iliac	no LNA	no LNA
19	MCT	R forearm	R ventral cervical R axillary	R prescapular	R prescapular	R prescapular
20	MCT	I L mammary gland	L axillary	L axillary L accessory axillary	L axillary L accessory axillary	L axillary L accessory axillary
21	MCT	nasal planum	R/L submandibular	R/L submandibular	R/L submandibular	R/L submandibular
22	MCT	R stifle	R inguinal	R inguinal * R medial iliac	R inguinal * R medial iliac	R inguinal *

23	MCT	L thigh - laterocaudal	L inguinal	L inguinal	L inguinal	L inguinal
24	MCT	tail - R lateral base	R lateral sacral R hypogastric	R medial iliac	R medial iliac	R medial iliac
25	MCT	preputium - R lateral	R inguinal	R/L inguinal	R/L inguinal	R/L inguinal
26	MCT	sternum - L lateral	L axillary	L prescapular	L prescapular	L prescapular
27	Melanoma	mandibular symphysis	R/L submandibular	L submandibular	L submandibular	L submandibular
28	MCT	R stifle	R inguinal	R inguinal	R inguinal R popliteal	R inguinal R popliteal
29	Parotid Adenocarcinoma	L parotid gland	L parotid L submandibular	L submandibular L parotid	L submandibular L parotid	NP
30	MCT	thorax - L lateral	L axillary	L accessory axillary	L accessory axillary	L accessory axillary
31A	MCT	R thigh - lateral	R inguinal R medial iliac	R inguinal	R inguinal	R inguinal
31B	MCT	head - L dorsolateral	L dorsal cervical L parotid	L prescapular	L prescapular x2	NP
31C	MCT	abdomen - L ventrolateral	L axillary	L accessory axillary	L accessory axillary	NP
32	Thyroid Carcinoma	R thyroid	R submandibular R dorsal superficial R retropharingeal	none	none	NP
33	SCC	sublingual	R/L submandibular R/L retropharingeal	R submandibular R/L retropharingeal	R submandibular R/L retropharingeal	L submandibular R/L retropharingeal
34	MCT	L foot	L popliteal	L popliteal	L popliteal	L popliteal
35	Benign Mammary Tumor	I L mammary gland	L axillary	L accessory axillary	L accessory axillary	L accessory axillary
36	Thyroid Carcinoma	R thyroid	R submandibular R dorsal superficial R retropharingeal	none	none	none
37	MCT	L ear base	L dorsal cervical L parotid	L prescapular	L prescapular	none
38	Melanoma	R oral vestibule	R submandibular	R submandibular	R submandibular	R submandibular
39	Mammary Carcinoma	III-IV L mammary gland	L axillary L inguinal	L inguinal	L inguinal	L inguinal
40	Sarcoma	L mandible	L submandibular	L submandibular	L submandibular	L submandibular
41A	Mammary Carcinoma	IV R mammary gland	R inguinal	R inguinal R medial iliac	R inguinal R medial iliac	R inguinal R medial iliac
41B	Mammary Carcinoma	V R mammary gland	R inguinal	R inguinal R medial iliac	R inguinal R medial iliac	R inguinal R medial iliac
42	MCT	L thigh - medial	L inguinal	L inguinal	L inguinal	L inguinal
43	PWT	L thigh	L inguinal L medial iliac	medial iliac	no LNA	no LNA

44	MCT	first sternebra	R/L axillary R/L ventral cervical	R/L prescapular	NP	L prescapular
45	MCT	L elbow	L axillary	L prescapular	L prescapular	none
46	MCT	L tibia cranio-medial	L inguinal	L inguinal L popliteal	NP	L inguinal L popliteal
47	MCT	L caudal ear base	L dorsal cervical	L prescapular	L prescapular	L prescapular
48	MCT	sternum - L cranio lateral	L axillary L ventral cervical	L prescapular	L prescapular	none
49	MCT	sternum - L lateral	L axillary	L accessory axillary	L accessory axillary	L accessory axillary
50	MCT	R proximal antebrachium	R ventral cervical	R prescapular R axillary	R prescapular R axillary	R prescapular R axillary
51	MCT	III digit L hand	L ventral cervical	L prescapular	L prescapular	NP
52	SCC - recurrence	mandibular symphysis	R/L submandibular	L submandibular	L submandibular	L submandibular

2.4 Discussion

This prospective study demonstrates the feasibility, safety, and efficacy of preoperative lymphoscintigraphy for SLN mapping in dogs with malignant tumors. Peritumoral injection of ^{99m}-Tc-labeled nanocolloids allowed for rapid detection of the SLN and the associated lymphatic pathway in 57/60 cases, without any injection-induced local reactions or systemic side effects.

Randall et al. recently reported a 100% SLN detection rate with lymphoscintigraphy in 20 dogs with head and neck malignancies *(Randall et al., 2020)*. In our study population, lymphoscintigraphy failed to identify SLN in 3 dogs, two of which had thyroid carcinoma. Successful detection of SLN in dogs with thyroid neoplasia has been previously described *(Balogh et al., 2002)*. In our investigation, one dog had a palpable thyroid carcinoma and received a peritumoral radiotracer injection which showed local activity diffusion without any lymphatic vessels or node detection. This failure could be due to the radiotracer diffusion within the cervical visceral space rather than the subcutaneous tissue. The second patient received an intratumoral ultrasound-guided radiotracer injection, as described in human oncology *(Gelmini et al., 2018)*, but no lymphatic drainage could be detected within one hour of the injection. In human patients with thyroid tumors, lymphoscintigraphy is performed up to 2 hours after the radionuclide injection *(Gelmini et al., 2018)*; therefore, a possible source of error may have been the short timing between the radiotracer injection and image acquisition. In the present study, lymphoscintigraphy was performed immediately before surgery and the dog was moved in the operating theater to avoid prolonging the duration of general anesthesia. Further studies are warranted to assess whether the migration of the radiotracer requires a longer time in thyroid tumors and to define a specific thyroid SLN mapping protocol for small animals. The third patient in which lymphoscintigraphy failed to identify the SLN, presented with an MCT recurrence. The patient also underwent prescapular lymphadenectomy during the first surgical session and adjuvant radiation therapy for nodal metastasis. In humans, the impact of scar tissue on SLN detection is controversial. Few studies have reported decreased SLN identification rate in patients where the lymphatic network was disrupted by a previous surgery *(Tada et al., 2005; Nowikiewicz et al., 2020)* or radiotherapy *(Lissidini et al., 2019).* Hlusko et al. *(2020)* investigated the impact of surgery on the drainage patterns from the canine brachium, demonstrating a partial agreement between preoperative and postoperative lymphoscintigraphy, and Vasques et al. *(2011)* showed that para-areolar incision in the upper outer quadrant of the first mammary gland did not significantly interfere with SLN identification in a canine model. However, both studies were conducted on healthy dogs, and data on tumor-bearing dogs is still lacking. Possible factors influencing the SLN detection rate in these cases are the interval between surgery and the successive SLN mapping procedure, formerly resected tissue volume and location, the tracer IS, and previous radiotherapy. Nonetheless, the affirmed ASCO guidelines still recommend SLN biopsy for this group of patients *(Lyman et al., 2017)*. For the dog in our study, the SLN could be identified with an MB peritumoral injection. Radiotracer failure could be attributed

to an error in the radiopharmaceutical preparation, in the image analysis, or due to the different tracer absorption levels. However, the presence of an inguinal radioactive, blue-stained connective tissue structure in another dog, that had previously undergone mastectomy (n = 22), further confirmed the abnormal tracer uptake in the presence of disrupted lymphatic drainage due to an old surgical scar.

Early dynamic images in the preoperative lymphoscintigraphy protocol did not offer additional clinical information on SLN detection, compared to static images, which is in line with previous research in human literature *(Lee et al., 2002)*. After the first appearance of the SLN on the dynamic or static images, orthogonal views need to be combined to correctly identify the SLN basin. To overcome the lack of anatomical details provided by lymphoscintigraphy, a syringe with a residual radiopharmaceutical was used as a pointer, as previously described *(Balogh et al., 2002; Pereira et al., 2008)*. Under the guidance of real-time images displayed on the gamma camera P-scope, the position of the pointer in relation to patient anatomical landmarks allowed the identification of the SLN basin. Although not used in this study, cobalt body markers or systemic administration of ^{99m}-Tc could further improve SLN identification, providing the visualization of body contour *(Pereira et al., 2008)*.

The differences observed in the SLN identification timing could be attributed to individual variations in lymphatic flow velocity as well as the animal's position and the subsequent effect of the bodyweight on tissues *(Randall et al., 2020; Majeski et al., 2017)*. This was not investigated in the current study and requires further research. The close proximity between the IS and the SLN basin can also lead to a challenging visualization of the LN uptake ("*shine-through*", *Siddique et al., 2018*). The use of a 2 mm lead shield to cover the IS markedly improved SLN visualization and reduced the concealing of the highly radioactive site on nearby nodes. However, in two dogs (n = 16 and 18) with an MCT of the right stifle, the intraoperative gamma probe identified an additional radioactive LN in the popliteal basin, which was not identified with lymphoscintigraphy, probably due to superimposition between the IS and the LN. In another patient with sub-lingual SCC (patient n. 33), MB identified an additional LN in the contralateral mandibular basin, which was not radioactive but was metastatic. In breast cancer patients, the failure of SLN identification is linked with an increased risk of metastases to the axillary lymph system *(Nowikiewicz et al., 2020)*. Recently, Rossi et al. *(2018)* described the failure of LN contrast uptake, using computed tomography lymphography, in cases with nodal macrometastasis. These findings highlight the importance of case selection among patients with clinically negative RLN and the combination of two mapping techniques (radiopharmaceutical and blue dye injection) to improve the SLN detection rate.

The study results confirm the hypothesis that the first LN draining the tumor site could be identified within unexpected lymphatic basins. Furthermore, lymphoscintigraphy allowed discrimination of the draining LN in cases where the tumor site was borderline between different lymphosomes or located in the axillary lymphosome. As previously stated, *(Worley et al., 2012; Tuohy et al., 2009; Ferrari et al., 2020)*, SLN mapping is a keystone concept in canine oncological staging, improving patient prognostication and management as it allows

for the correct adjuvant therapy suggestion and has a therapeutic role in MCT tumors *(Marconato et al., 2020).*

An important limitation of scintigraphy is the need for authorization and equipment for radioactive isotope use, which limits the number of facilities with nuclear medicine services. In addition, specific precautionary procedures are required to guarantee personnel safety, despite radiation exposure being reported to be minimal *(Worley et al., 2012)*. As a consequence, other SLN mapping techniques have been developed in human medicine and further described for oncological staging purposes in dogs, such as the radiographic lymphography *(Brissot et al., 2017)*, computed tomography lymphography *(Randal et al., 2020; Majeski et al., 2017; Rossi et al., 2018; Soultani et al., 2017; Grimes et al., 2020),* contrast-enhanced ultrasound *(Lurie et al., 2006; Fournier et al., 2020)*, and near-infrared imaging *(Reynolds et al., 1999; Beer et al., 2019)*.

To the best of our knowledge, this study is the largest cohort of dogs undergoing radiopharmaceutical SLN mapping for malignant tumor staging and provides the first description of the procedure in a feline patient in a clinical setting. A limitation of this study is the application of a canine lymphosome map to a feline patient. A literature review identified a study by Wong et al. that investigated the inguinal lymphatic drainage in a feline model *(Wong et al., 1991)*. Additional studies are needed to create a complete feline lymphatic territory map and to explore the SLN mapping technique in cats after this first experience.

In conclusion, preoperative planar lymphoscintigraphy is a feasible, safe, and effective method for SLN detection in dogs with spontaneous malignancies in different anatomical locations. This mapping technique drives the surgical extirpation of SLNs in a specific lymphocentrum, allowing for accurate oncologic staging, either for identifying the tumor-draining node within unexpected lymphatic basins or discriminating the draining node in uncertain cases. The use of combined preoperative and intraoperative techniques is recommended to improve the SLN detection rate.

3. Feasibility of SPECT and CT image fusion (SPECT/CT) for sentinel lymph node imaging in veterinary oncology.

Abstract

Single proton emission computed tomography/Computed Tomography (SPECT/CT) is a dual modality imaging method that combines functional and morphological studies, overcoming the drawbacks of both modalities and accentuating their advantages. In human medicine, this hybrid technique proved to increase the SLN detection rate identifying lymph nodes that were missed on planar images and providing detailed anatomical information. In this prospective observation study, we evaluate the feasibility and clinical value of SPECT/CT images fusion using an opensource software for multimodality medical images analysis (AMIDE) in 25 dogs with spontaneous malignant tumors undergoing SLN mapping procedure. Images of SPECT and CT scans could be successfully merged in 21 of the 25 dogs due to correct patient positioning. In 18 cases there were a perfect agreement between the SLNs identified on planar and SPECT/CT images, while in 3 dogs the nodal hotspot was clearly identified in SPECT alone, but not on fused SPECT/CT images, probably due to the injection site *shine-through* effect. The success of the images merging is strictly related to patients positioning. Further studies are needed to assess the clinical relevance of SPECT/CT combined imaging modality for SLN mapping in veterinary oncology.

3.1 Aim of the study:

The aim of this study was to evaluate the feasibility and clinical value of merging Single Proton Emission Computed Tomography (SPECT) lymphoscintigraphy with Computed-Tomography (CT) images for sentinel lymph node (SLN) mapping in veterinary oncological patients. We compared planar images and SPECT/CT fused images for sentinel lymph nodes anatomical localization in dogs with spontaneous malignant tumor.

3.2 Materials and methods

Client-owned dogs presenting for surgical resection of a primary malignant tumor were enrolled in this prospective observational study. The inclusion criteria were as follows: (a) Cytologically or histologically confirmed malignant tumor, (b) Tumor mass amenable for peritumoral tracer injection (c), No-palpable or clinically unaltered (symmetrically palpable in the contralateral lymphatic basin) regional lymph nodes, and (d) Absence of distant metastasis at admission, according to the staging reference guidelines for each tumor (three views thoracic radiographs and abdominal ultrasound with cytology of spleen and liver, or whole-body contrast-enhanced CT). All the procedures were conducted following the European legislation concerning Animal Protection and Welfare (Directive 2010/63/EU) and the Italian ethical law (Decreto Legislativo 04/03/2014, n.26). A client-signed informed consent was obtained for every procedure. Each animal received blood testing and presurgical workup according to the type of neoplasia, comorbidities and/or presenting clinical signs.

Preoperative Planar lymphoscintigraphy, SPECT and CT

Lymphoscintigraphy was performed with dogs under general anesthesia. A ^{99m}-Technetium (^{99m}-Tc) labeled nanosized human serum albumin (NANOALBUMON, Radiopharmacy Laboratory Ltd., Budaörs, Hungary) solution was prepared using 0.9% NaCl as a solvent. Each patient received a radiopharmaceutical injection (8-35 MBq/0.5 ml), in 4 quadrants around the tumor with a 25-G needle, and a systemic ^{99m}-Tc pertechnetate solution (32-60 MBq/1 ml) administration to provide the visualization of body contour. The MBq dose of the syringes was measured using a dose calibrator (ATOMLAB 100Plus, Biodex Medical Systems, Shirley, New York), before and after the systemic and peritumoral injection to calculate the administered dose. Orthogonal planar static images (120s/frame, matrix size 256x256) were acquired within few minutes after the injection with a single-head gamma camera (Picker Prism 1000XP, Picker International, Highland Heights, Ohio, USA), until the SLN was clearly identify. If needed, the injection site was masked with a 2 mm-thick lead shield of appropriate size to reduce the associated *shine-through* effect.

After planar images acquisition, a SPECT scan was performed with the same single-head gamma camera. Dogs were placed in dorsal recumbency using a hard cradle CT positioner. If

a dog underwent contrast-enhanced CT for tumor staging before lymphoscintigraphy, it was placed for the SPECT scan in the same CT positioning conditions. Data acquisition was performed with a 128x128 matrix size and a 360° orbit, acquiring 120 frames (10 s/step), one every 3° angular step, in a continuous motion type. The total acquisition time was 20 min. Dogs were then transported to CT imaging room with the cradle to maintain the same positioning for both modalities. A regional CT scan was performed using a 16-slice helical scanner (GE *BrightSpeed Elite*, GE Healthcare, Milwaukee, WI, USA). The acquisition protocol included soft tissue algorithm with tube rotation time 1 s, slice thickness 1.25, collimator pitch 0.937, tube voltage set at 100 or 120 kVp, and tube current ranged from 180 to 200 mAs based on patient size. The CT scan was not repeated in dogs which previously underwent contrast-enhanced CT for tumor staging at our institution. Animals recovered from anesthesia and were hospitalized and monitored for the night.

Intraoperative SLN detection

The day after preoperative SLN mapping, dogs were admitted to surgery for tumor excision and SLN extirpation. Prior to the aseptic preparation of surgical site, 0.4 ml solution of 5mg/ml sterile methylene blue (S.A.L.F. S.p.A, Cenate Sotto, Bergamo, Italy) was injected in 4 quadrants around the primary tumor. A handheld gamma probe (Crystal probe SG04, Crystal Photonic GmbH, Berlin, Germany) was used to guide the surgical dissection during the lymphadenectomy procedure. Any lymph node presenting blue stain or a radioactive count at least double than background, was extirpated. Primary tumor and extirpated LN were checked *ex vivo* with the detector and then fixed in 10% neutral-buffered formalin for a routine histopathological examination.

SPECT/CT image fusion technique

Three-dimensional images fusion of SPECT and CT scans were obtained using AMIDE, an opensource software for viewing, analyzing, and registering volumetric medical imaging data sets (Amide's a Medical Image Data Examiner; *amide.sf.net*) *(Loening, 2001; Loening, 2003)*. For SPECT images, a three-plane transverse image reconstruction was obtained using the nuclear medicine workstation (Odyssey FX, Picker International, Highland Heights, Ohio, USA) and used for images fusion. Both modalities data were imported in the fusion software as Digital Imaging and Communications in Medicine (DICOM) files. The CT and SPECT images were superimposed on AMIDE viewer in three planes – transverse, sagittal and dorsal slices. By manually moving the SPECT images over CT, we adjusted the body contours to overlap as correctly as possible and we used the dog primary tumor as a fiducial marker for images alignment. After images reconstruction, the nodal uptake identified with SPECT/CT was compared to the SLN detected with planar lymphoscintigraphy.

3.3 Results

Twenty-five dogs with 26 malignancies were included in the study. Median age was 8.4 ±3.4 years (range: 1 – 13 years) and median weight 25 ±11.25 kg (range: 6 – 44 kg). Thirteen dogs were males, of which 3 neutered, while 12 dogs were female, of which 9 spayed. After mixed breed dogs (7), the most represented breeds were Labrador retriever (4) and English setter (4), followed by Pug (2) and one each of: American Staffordshire, Weimaraner, Fox terrier, Setter Gordon, Tibetan terrier, Flat coated retriever, Bernese mountain dog, and Bull terrier. Included neoplasia were mast cell tumor (MCT, 20), oral melanoma (2), mandibular osteosarcoma (1), thyroid carcinoma (1), malignant mesenchymoma (1), and hepatoid glands carcinoma (1). One dog presented with two MCTs, one at the right stifle and the other on the prepuce. Both tumors underwent preoperative SLN mapping procedure at the same time. Details on dogs signalment, tumor sites and identified SLNs are shown in Table 3.1.

Images of SPECT and CT scan could be successfully merged with AMIDE in 21 out of 25 dogs. Those cases where the one in which the CT scan was carried out immediately after SPECT and included all the dogs with MCTs. In the other 4 cases, contrast enhanced-CT was performed two (1) and three (1) weeks before SLN mapping for staging purposes, or right before preoperative lymphoscintigraphy (2). The differences in patients positioning prevent a correct images fusion, with only a partial (2) or no match (2) between the nuclear images' nodal hotspots and the CT lymphatic basins. In 18 cases where a successful images fusion was accomplished, there were a perfect agreement between the SLNs identified on planar images and hot lymphatic basins on SPECT/CT images. In the other 3 dogs, the nodal hotspot was clearly identified in SPECT alone, but not on fused SPECT/CT images, where the uptake was too faint, regardless the selected image threshold.

Complete SLN mapping procedure with preoperative planar lymphoscintigraphy, SPECT and two intraoperative techniques was performed in 20 cases, while methylene blue injection was not employed in 4 dogs and the handheld gamma probe was not used in one case.

There was a complete agreement on the identified SLN among preoperative and intraoperative techniques in 21 cases (84%). In the dog with thyroid carcinoma, only preoperative techniques identified the SLN while no hot or blue nodes were identified during surgery. The blue dye did not stain any lymph nodes in other 2 cases and partially identified the SLNs in the dog with hepatoid glands carcinoma. In one dog with an MCT of the ventral thoracic wall, there was a partial match between the lymph nodes identified with preoperative technique and the intraoperative gamma probe. This dog previously underwent chemotherapy for lymphoma.

Lymphadenectomy was performed in all cases and a total of 48 lymph nodes were extirpated, with a mean of 1.8 lymph nodes per tumor, ranging from 1 lymph node (14 tumors) to 9 nodes in the dog with hepatoid glands carcinoma. Regarding MCTs, histopathological examination revealed absence of metastases (HN0) in 6/19 dogs, pre-metastatic nodal lesion (HN1) in 3/19 dogs, early metastases (HN2) in 7/19 dogs, and overt metastases (HN3) in 3/19 dogs. As for the other malignancies, 3/6 dogs presented nodal metastases (2 oral melanoma, 1 hepatoid glands carcinoma).

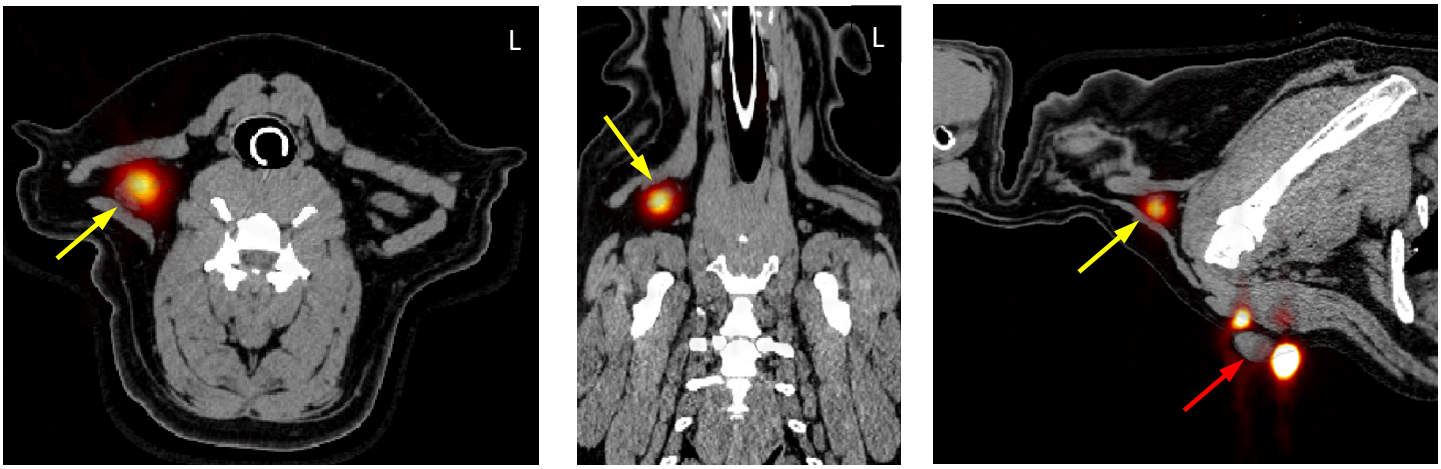

Figure 3.1. Transverse, dorsal, and sagittal SPECT/CT fused images of a dog with mast cell tumor at the right-ventral thoracic inlet (injection site, red arrow) drained by right cervical superficial lymph node (SLN, yellow arrow).

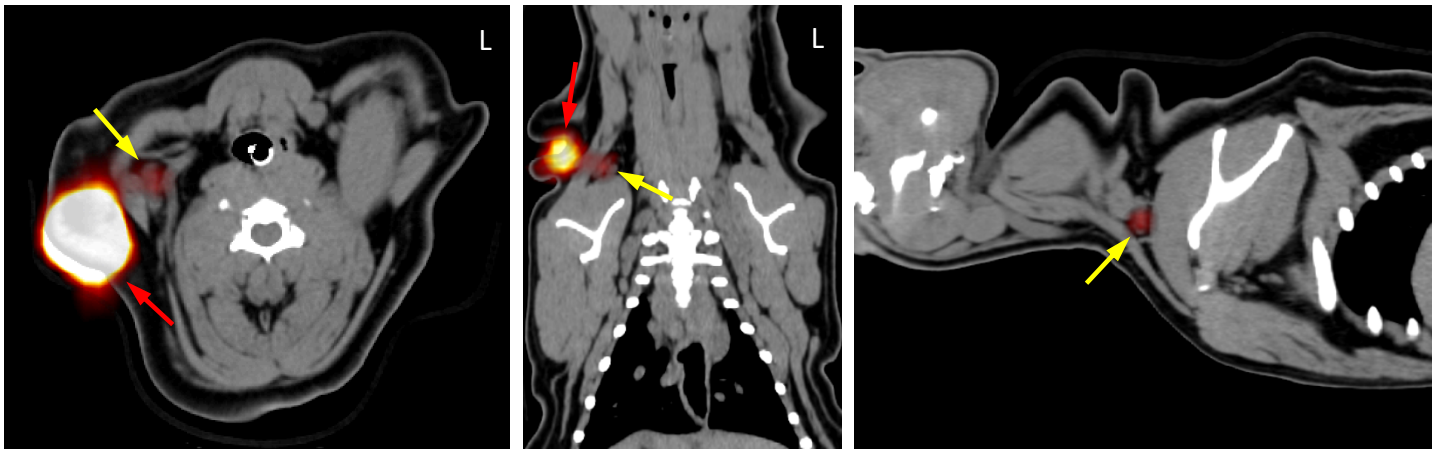

Figure 3.2. Transverse, dorsal, and sagittal SPECT/CT fused images of a dog with mast cell tumor at the right-caudal neck (injection site, red arrow) which is superimposed to the draining right cervical superficial lymph node (SLN, yellow arrow).

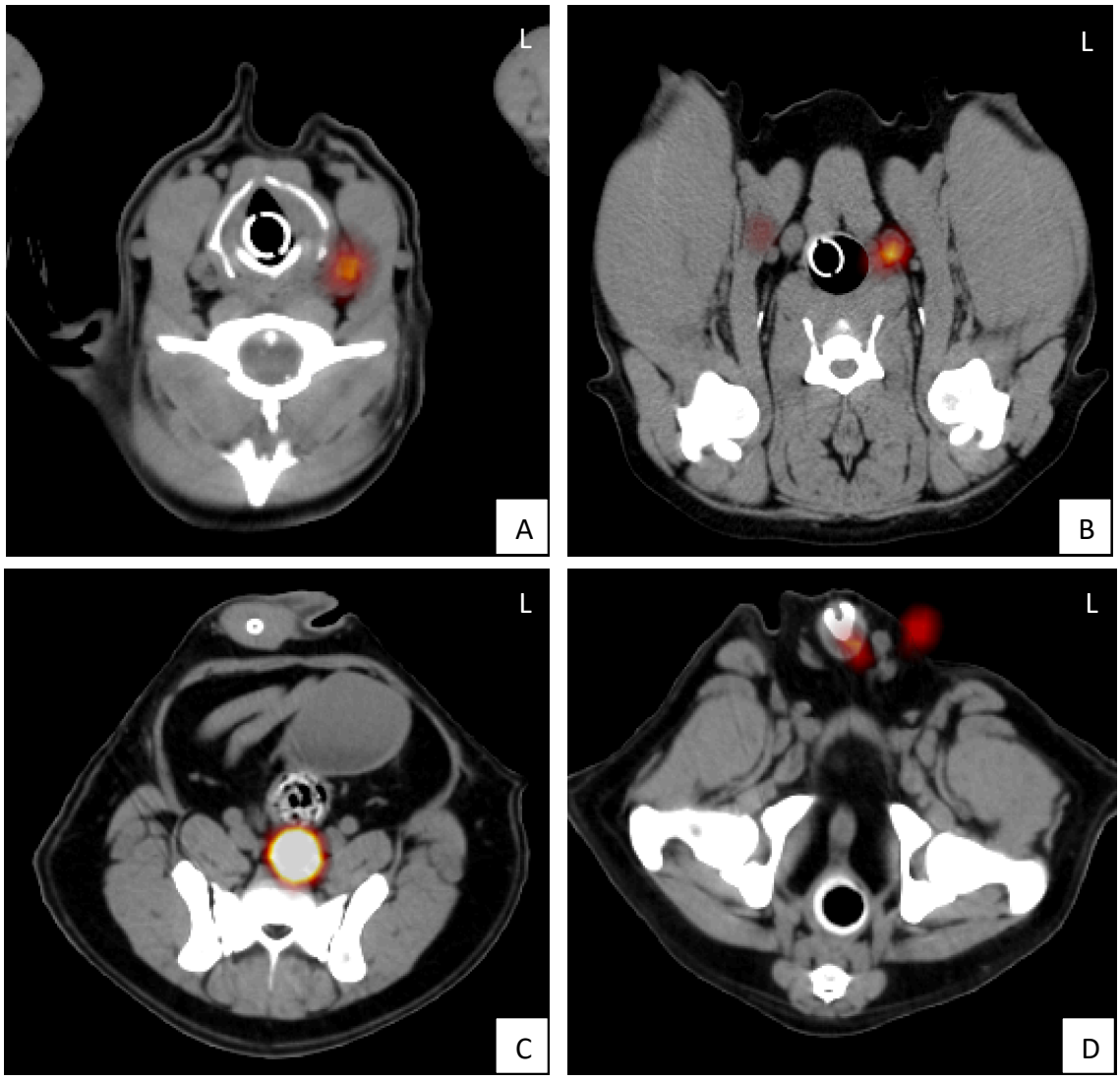

Figure 3.3. Failed SPECT/CT images fusion in two dogs with left thyroid carcinoma (A, B) and hepatoid gland carcinoma (C, D). In both cases only a partial images correspondence was obtained with successful overlapping of the left retropharyngeal (A) and internal iliac (B) lymph nodes. The other visible hotspots could not be correctly superimposed to CT lymphatic basins (B, D).

Table 3.1 Signalment (breed, sex, age, weight), tumors type and site, identified SLNs with lymphoscintigraphy and intraoperative techniques, and lymph nodes histopathology results of the 25 dogs enrolled in this study. For mast cell tumors, lymph node classification according to Weishaar et al. *(2014)* have been reported.
Abbreviations: M, male; F, female; n, neutered; R, right; L, left.

	Breed	Sex	Age (years)	Weight (kg)	Tumor type	Tumor site	Lymphoscintigraphy	Gamma probe	Methylene blue	LN metastases
1	AmStaff	Fn	12	31.7	Mast cell tumor	L armpit	L axillary	L axillary	Not performed	no (HN0)
2	Weimaraner	Mn	8	37.25	Mast cell tumor	R thigh	R inguinal	R inguinal	R inguinal	yes (HN2)
3	Fox Terrier	Fn	9	8,1	Mast cell tumor	R dorsal head	R cervical superficial	R cervical superficial	Not performed	yes (HN2)
4	Pug	M	7	8.8	Mast cell tumor	R caudal neck	R cervical superficial	R cervical superficial	Not performed	no (HN1)
5	Mixed breed	M	13	26.8	Mast cell tumor Mast cell tumor	R stifle Prepuce	R inguinal R and L inguinal	R inguinal R and L inguinal	R inguinal R and L inguinal	yes (HN2)
6	Setter gordon	M	9	18.5	Mast cell tumor	R thigh	R inguinal	R inguinal	R inguinal	yes (HN2)
7	Tibetan Terrier	M	2	10	Mast cell tumor	L eye conjunctiva	L parotideal	L parotideal	None	no (HN0)
8	Mixed breed	Fn	9	33.6	Mast cell tumor	R stifle	R inguinal	R inguinal	R inguinal	no (HN0)
9	Labrador retriever	M	3	41	Mast cell tumor	L caudal neck	L cervical superficial	Not performed	L cervical superficial	no (HN1)
10	Flat Coated retriever	Fn	11	28	Thyroid carcinoma	Left thyroid lobe	L retropharyngeal L and R cervical superficial	None	None	no
11	English Setter	Fn	6	17	Mast cell tumor	R shoulder	R cervical superficial	R cervical superficial	R cervical superficial	no (HN0)
12	English Setter	Mn	8	18	Mast cell tumor	R thorax	R accessory axillary	R accessory axillary	R accessory axillary	yes (HN2)
13	Mixed breed	M	9	27.8	Mast cell tumor	Prepuce	R and L inguinal	R and L inguinal	R and L inguinal	yes (HN3)
14	Labrador retriever	M	12	36	Oral melanoma	R superior labium	R mandibular	R mandibular	R mandibular	yes
15	Pug	F	12	6	Mast cell tumor	L thigh	L inguinal	L inguinal	L inguinal	no (HN0)
16	Labrador retriever	Mn	10	44	Mast cell tumor	R thoracic inlet	R cervical superficial	R cervical superficial	R cervical superficial	yes (HN2)
17	English Setter	Fn	12	19.6	Mast cell tumor	L caudal neck	L cervical superficial	L cervical superficial	Not performed	yes (HN2)
18	Mixed breed	Fn	11	10.5	Osteosarcoma	R hemimandibula	R and L mandibular L retropharyngeal	R and L mandibular L retropharyngeal	R and L mandibular L retropharyngeal	no
19	English Setter	F	1	15	Mast cell tumor	R third eyelid	R parotideal	R parotideal	R parotideal	yes (HN3)
20	Mixed breed	M	8	35	Oral melanoma	L superior labium	L mandibular	L mandibular	L mandibular	yes
21	Bernese Mountain dog	Fn	4	38	Malignant mesenchymoma	R cranial neck	R cervical superficial	R cervical superficial	R cervical superficial	no
22	Bull Terrier	M	4	29.2	Mast cell tumor	R scrotum	R inguinal	R inguinal	R inguinal	no (HN0)
23	Labrador retriever	Fn	12	32	Mast cell tumor	R ventral thorax	R cervical superficial R axillary	R cervical superficial	None	no (HN1)
24	Mixed breed	M	10	31.6	Hepatoid gland carcinoma	Circumanal	internal iliac sacral R medial iliac L inguinal	internal iliac sacral R medial iliac L inguinal	L sacral	yes
25	Mixed breed	F	9	23.2	Mast cell tumor	R shoulder	R cervical superficial	R cervical superficial	R cervical superficial	yes (HN3)

3.4 Discussion

To our knowledge, the present study reports for the first time the feasibility of SPECT/CT images fusion for SLN mapping in dogs with spontaneous malignancies in a clinical setting.
Single photon emission computed tomography is a tomographic technique in which the three-dimensional images of radioactive tracer distribution in tissues is produced through the detection of single-photon emissions from the radionuclides introduced into the body. Lymph node-scintigrams acquired either as planar or SPECT images for SLN mapping show lack of anatomical detail or references landmarks, because the radiopharmaceutical is only found in the lymphatic system. In our study, the systemic administration of a radionuclide solution provided the visualization of body contour which improved anatomical landmarks identification both in planar images, as previously described *(Pereira et al., 2008)*, as well as in SPECT scan. On the other hand, CT is a tomographic technique which uses an external X-ray source to produce detailed three-dimensional anatomic images. SPECT/CT is a dual modality imaging method that combines functional and morphological studies, overcoming the drawbacks of both modalities and accentuating their advantages. Image fusion software, such as AMIDE, can assemble a merged image from SPECT and CT scans without the need of expensive SPECT/CT hybrid imaging systems. In the present study, the fusion of SPECT/CT images was successfully accomplished in 21 dogs. All these patients underwent firstly SPECT scan then CT examination, maintaining the same positioning for both imaging modalities. This allowed an accurate superimposition between images in all three planes - transverse, sagittal and dorsal. In the other 4 dogs, contrast enhanced-CT was performed prior to SLN mapping procedure in order to correctly stage the canine patient and fulfil inclusion criteria excluding the presence of distant metastases. Those differences represent a limitation in this study, however we decided to not repeat the CT after lymphoscintigraphy in order to reduce the dog radiation exposure.
Besides feasibility, the clinical relevance of SPECT/CT images in SLN mapping should be discussed. In human literature, the data provided by SPECT/CT images were concluded to be clinically relevant if this technique identified lymph nodes that were missed on planar images, if it excluded a suspected SLN on planar images, or if it localized the SLN in different lymphatic basins than those suggested by planar lymphoscintigraphy *(Even-Sapir et al., 2003)*. For breast cancer, this hybrid mapping technique proved to increase the SLN identification rate in overweight and obese patients, in patients with non-visualization of the lymph node on planar images, in patients with an unusual drainage pattern and in patients with difficult-to-interpret images *(Wagner et al., 2013)*. In this study, we observed perfect agreement between the lymph nodes identified with planar lymphoscintigraphy and the ones visualized on SPECT/CT images. Therefore, the clinical relevance of SPECT/CT combined imaging modality for SLN mapping in veterinary oncology needs to be further evaluated, for example assessing its utility in surgical planning. Furthermore, SPECT/CT seems to be of most use for tumors localized in complicated anatomical regions, such as head and neck, which are not appropriately rendered on planar imaging *(Wagner et al., 2013)*. In our cohort of dogs, 11 animals presented

with head and neck malignancies and in 3 cases SPECT/CT images fusion was not possible due to patient mispositioning, highlighting the complexity of this region. The fourth dog in which SPECT/CT images fusion failed, was a patient presenting with hepatoid gland carcinoma. The pelvic region is another challenging area with a high density of lymphatic basins (e.g., sacral, medial iliac, internal iliac). In this dog, the lymph nodes identified with planar lymphoscintigraphy were internal iliac, sacral, right medial iliac and left inguinal node. The attempted SPECT/CT images fusion showed a hotspot on the right medial iliac and internal iliac lymph nodes, which appeared mildly enlarged on CT, and apparent bilateral uptake of inguinal lymph nodes, even if not correctly superimposed to CT images, probably due to a different placement of the penile body *(Fig. 3.3)*. A possible SLN (left inguinal) missed on planar images could have been detected, but because of patient mispositioning it was not possible to confirm this finding. However, the intraoperative techniques did not identify the left inguinal node. Nonetheless, in another patient preoperative and intraoperative techniques disagree on SLN detection. In fact, in the dog presented with thyroid carcinoma preoperative lymphoscintigraphy identified the left retropharyngeal and both cervical superficial lymph nodes as the ones which drains the tumor site, but no hot or blue node were found with intraoperative techniques. The reason behind this discrepancy remains unclear. The challenges in SLN mapping in dogs with thyroid tumors has been also highlighted in the previous study of this PhD dissertation. Regarding SPECT/CT images fusion, this patient underwent staging contrast-enhanced CT two weeks before SLN mapping procedure, and even if both exams were performed in ventral recumbency, the position of the forelimbs was not identical and only the left retropharyngeal nodal uptake could be correctly superimposed on CT images. A partial match between preoperative and intraoperative techniques was found in a dog with an MCT of the ventral thoracic wall, which previously underwent chemotherapy for lymphoma. In this patient, both planar and SPECT/CT fused images showed a radiopharmaceutical uptake in the axillary space, but no lymph nodes were recognized in this region with intraoperative gamma probe and only the cervical superficial homolateral node was excised. Besides previous surgery and radiotherapy, mentioned in our first study, even chemotherapy is reported as a possible risk factor for lymphoscintigraphic failure, due to lymphatic network disruption and nodal *changes (Lissidini et al., 2019)*.

An additional reported advantage of SPECT/CT images is an increase visualization of nodes not seen or only suspected on planar imaging due to injection site *shine-through* artifact and superimpositions *(Lerman et al., 2016)*. In three patients, the nodal hotspot was clearly identified in SPECT alone, but not on the merged SPECT/CT images, where the uptake was too faint, regardless the selected image threshold. The scattering of gamma rays impairs the visualization of hot lymph nodes when they are located close to the injection site. The application of filters and pixel truncation could exclude the effects of high levels of activity at the injection site, reducing the artifacts and improving lymph nodes identification *(Kizu et al., 2005)*.

In conclusion, we demonstrated the feasibility of SPECT and CT images fusion in dogs with spontaneous malignancies undergoing SLN mapping procedures. The success of the images

merging is strictly related to patients positioning, which could be further improved using external fiducial markers. Further studies are needed to assess the clinical relevance of SPECT/CT combined imaging modality for SLN identification in veterinary oncology.

4. Comparison between computed tomography indirect lymphography and lymphoscintigraphy for SLN mapping in dogs with mammary tumor: preliminary results.

Abstract

Mammary gland tumor is one of the most common neoplasia in canine patients. In particular, mammary carcinoma metastasizes at distance via the lymphatic system, therefore the sentinel lymph node (SLN) assessment significantly impacts the oncological staging of the disease. Different techniques have been described for SLN mapping in bearing tumor dogs.

This report presents the preliminary results of a prospective ongoing study comparing computed tomography (CT)-indirect lymphography to planar lymphoscintigraphy and intraoperative techniques for SLN detection in dogs with mammary tumors. In the first five cases, at least one lymph node was identified in each dog by every technique, but it was a complete match only in 2 dogs (40%). The number of identified lymph nodes differed based on the SLN mapping modality, therefore the use of a combined detection technique is recommended to reduced false negative cases.

4.1 Aim of the study

We want to present the preliminary results of an ongoing study comparing two preoperative techniques, computed tomography (CT) and scintigraphy, and two intraoperative techniques, blue dye and handheld gamma probe, for SLN detection in dogs with mammary tumors. We hypothesize that both CT-indirect lymphography and planar lymphoscintigraphy would prove to be valuable techniques for SLN mapping and that the water-soluble iodinated contrast agent peritumorally injected for CT-indirect lymphography would identify the same lymph nodes when compared to radiocolloids and blue dye.

4.2 Materials and methods

Patients

Client-owned dogs presenting for mammary tumor surgical resection were prospectively enrolled in this method-comparison study. The inclusion criteria were as follows: (a) cytologically confirmed malignant or borderline-malignancy mammary neoplasia, (b) no-palpable or clinically unaltered (symmetrically palpable in the contralateral lymphatic basin) regional lymph nodes, and (c) three views thoracic radiographs negative for metastasis. All the procedures were conducted following the European legislation concerning Animal Protection and Welfare (Directive 2010/63/EU) and the Italian ethical law (Decreto Legislativo 04/03/2014, n.26). A client-signed informed consent was obtained for every procedure. Each animal received blood testing and presurgical workup according to comorbidities and/or presenting clinical signs.

CT-indirect lymphography

Dogs were anaesthetized according to clinician preferences. Each patient underwent whole-body contrast-enhanced CT scan for routine mammary tumor staging using a 16-slice helical scanner (GE *BrightSpeed Elite*, GE Healthcare, Milwaukee, WI, USA). Dogs were placed in dorsal recumbency and CT images were obtained before and after intravenous administration of iodinated contrast media (iodixanol, dosage: 640 mgI/kg; Visipaque 320, General Electric Healthcare, Milan, Italy) injected into a cephalic vein through an IV catheter using a power injection (Medrad Mark V Plus, Soma Tech INTL, Bloomfield, CT, USA). The acquisition protocol included medium frequency reconstruction algorithm for soft tissue and high frequency algorithm for lung and bone. Tube voltage was set at 120 kVp, tube rotation time was 1 s, slice thickness was 1.25 or 2.5 mm, collimator pitch was 0.937 or 1.375, tube current ranged from 180 to 200 mAs based on patient size. After contrast-enhanced CT, indirect lymphography was performed. A water-soluble iodinated contrast agent (iomeprol, Iomeron, 300 mgI/mL, Bracco Imaging., Milano, Italy) was injected using a 25-G needle in four quadrants around the tumor and gently massaged for 30 seconds. The amount of injected contrast agent depended on patient weight: <10 kg: 0.8 ml, 10-20 kg: 1.2 ml, >20: 2 ml, as

previously described *(Rossi et al., 2018)*. A 1.25 mm CT scan from thoracic inlet (including cervical superficial lymph nodes) to the sacrum (including inguinal lymph nodes) was acquired 1 minute after the injection. If needed, additional CT scan for SLN identification were repeated after 6, 9 or 12 minutes.

Planar lymphoscintigraphy

Lymphoscintigraphy was performed under general anesthesia, the same day or the day before surgery. A ^{99m}-Technetium labeled nanosized human serum albumin (NANOALBUMON, Radiopharmacy Laboratory Ltd., Budaörs, Hungary) solution was prepared using 0.9% NaCl as a solvent. Each patient received a peritumoral radiopharmaceutical injection (15-30 MBq/0.5 ml), in 4 quadrants around the mammary tumor with a 25-G needle, and a systemic ^{99m}-Tc pertechnetate solution (34-50 MBq/1 ml) in order to provide the visualization of animal body contour and allow anatomical landmarks identification. The MBq dose of the syringes was measured using a dose calibrator (ATOMLAB 100Plus, Biodex Medical Systems, Shirley, New York), before and after the systemic and peritumoral injection to calculate the administered dose. Orthogonal regional static images (120s/frame, matrix size 256x256) were acquired immediately after the injection with a single-head gamma camera (Picker Prism 1000XP, Picker International, Highland Heights, Ohio, USA) until the SLN was clearly identify. If needed, the injection site was masked with a 2 mm thick lead shield of appropriate size to reduce the *shine-through* effect and obtain a better identification of the lymphatic pathway.

Surgery

The same day or the day after lymphoscintigraphy, dogs were admitted to surgery for unilateral radical mastectomy and SLN extirpation. Prior to the aseptic preparation of surgical site, 0.4ml solution of 5mg/ml sterile methylene blue (S.A.L.F. S.p.A, Cenate Sotto, Bergamo, Italy) was peritumorally injected in the same fashion as the iodinated contrast agent and radiocolloids. A handheld gamma probe (Crystal probe SG04, Crystal Photonic GmbH, Berlin, Germany) was used to guide the surgical dissection during the lymphadenectomy procedure. Any lymph node presenting blue stain or a radioactive count at least double than background, was extirpated. The mammary chain and extirpated lymph nodes were fixed in 10% neutral-buffered formalin for a routine histopathological examination.

Data analysis

Data recorded and compared in the study included: number of identified SLNs with CT-indirect lymphography, planar lymphoscintigraphy, intraoperative handheld gamma probe and blue dye; agreement between lymph nodes detected with the four techniques; correspondence between the identified SLN and the expected one based on mammary tumor site. The agreement between the techniques was described as a complete match if the identified lymph node was the same, a partial match if there was only partial agreement

between the identified nodes, or no match in case of different lymph nodes identification. Inferential statistics were not performed due to the sample size.

4.3 Results

Preliminary results of the study include 5 bitches with mammary tumors. One dog has been excluded after staging CT examination, due to hepatic and musculoskeletal tumor metastatic spread. Breeds included 2 mixed breed dogs and one each of Italian hound, Lagotto romagnolo, Chihuahua. Two of the five bitches were spayed. Mean age was 8 ±2.5 years (range: 4-8), mean weight was 14 ±10.8 kg (range: 3.2-31 kg). Mammary tumors were distributed on the 4th (2 right, 1 left) and on the 5th (1 right, 1 left) gland, and the tumor size (longest diameter) ranged from 0.1 to 3.0 cm, with a mean of 2.6 ±0.6 cm.

Lymphoscintigraphy was performed on the same day of surgery in 4 dogs and the day before surgery in one case (dog n. 5). Each technique identified at least 1 lymph node in all dogs (*Table 4.1*). In particular, 7 lymph nodes were detected in the five dogs by CT-indirect lymphography, 10 lymph nodes were detected by lymphoscintigraphy, and 9 by intraoperative handheld gamma probe. Methylene blue was not used in one case and stained 8 lymph nodes in the remaining 4 dogs.

There was a complete match among all techniques in 2 out of 5 cases (dogs n. 1 and n. 4; 40%). This dogs both presented with neoplasia at the 5th mammary gland and only one lymph node (inguinal) was identified by all the techniques. Intraoperative handheld gamma probe and blue dye injection showed a complete match with each other in all the 4 cases where they were both performed. The three dogs with tumors localized at the 4th mammary gland all had a partial match among the four techniques. In one of this dogs, intraoperative techniques completely match with lymphoscintigraphy identifying the right inguinal and the right medial iliac lymph nodes, while CT-indirect lymphography detected only the inguinal lymph node. In the second partial match case, CT-indirect lymphography identified 2 lymph nodes, lymphoscintigraphy detect an additional lymph node while intraoperative techniques identified another additional node compared to lymphoscintigraphy, for a total of 4 SLN. The third dog (*Figure 4.1*) had 2 lymph nodes detected with CT-indirect lymphography, an additional lymph node identified with lymphoscintigraphy and only one lymph node detected with the handheld gamma probe.

The histopathological examination revealed no signs of nodal metastasis in all the extirpated lymph nodes. No side effects related to injected radiocolloids or methylene blue were observed, while one patient developed a small hematoma at the injection site after iodinated contrast agent injection.

Table 4.1. Results of mammary tumor distribution and the sentinel lymph nodes identified with CT-indirect lymphography, planar lymphoscintigraphy, intraoperative handheld gamma probe and methylene blue dye.
Abbreviation: CT-IL, computed tomography-indirect lymphography; L, left; R, right.

	Mammary gland	CT-IL	Lymphoscintigraphy	Gamma probe	Methylene Blue
1	5 Left	L inguinal	L inguinal	L inguinal	L inguinal
2	4 Right	R inguinal R axillary accessory	R inguinal R axillary accessory R medial iliac	R inguinal R axillary accessory R axillary R medial iliac	R inguinal R axillary accessory R axillary R medial iliac
3	4 Right	R inguinal	R inguinal R medial iliac	R inguinal R medial iliac	R inguinal R medial iliac
4	5 Right	R inguinal	R inguinal	R inguinal	R inguinal
5	4 Left	L inguinal L medial iliac	L inguinal L axillary accessory L medial iliac	L inguinal	*Not performed.*

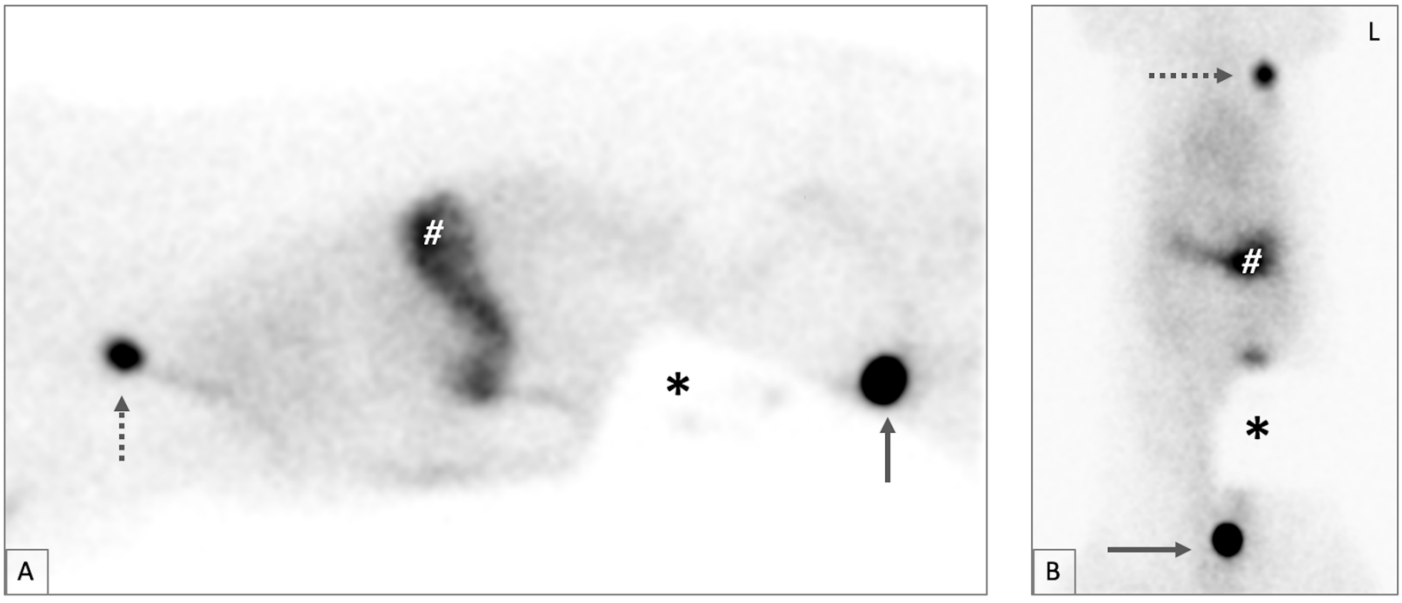

Figure 4.1. Lateral (A) and dorsal (B) images of preoperative planar lymphoscintigraphy (dog n. 5). The injection site (*) is masked with a lead foil to reduce the *shine-through* effect. Dotted arrow: left accessory axillary lymph node; full arrow: left inguinal lymph node. The gastric silhouette (#) is visible on both images due to mucosal uptake of systemic ^{99m}-Technetium.

4.4 Discussion

Preliminary results of this ongoing research show that the identified SLN varied among different mapping techniques in 3 out of five cases. Therefore, we reject the hypothesis that the water-soluble iodinated contrast agent peritumorally injected for CT-indirect lymphography would identify the same lymph nodes when compared to radiocolloids and blue dye. These findings are consistent with a recent method comparison study on healthy dogs which compared lymphoscintigraphy and radiographic indirect lymphography, describing partial or no match between techniques in 5 out of 8 dogs *(Hlusko et al., 2020)*.
In this study, discrepancy among techniques was found in dogs with tumor located at the 4th mammary gland, which is reported to be one of the glands most frequently affected by mammary neoplasia *(Sautet et al., 1992)*. In literature, different drainage patterns have been described for the caudal abdominal (4th) mammary gland in healthy bitches as well as in dogs affected by mammary tumor. In particular, a study on healthy dogs reported a greater variability in SLNs number and lymphatic draining patterns identified with lymphoscintigraphy compared to the other mammary glands *(Pereira et al., 2008)*. The identified lymph nodes in 5 dog's caudal abdominal mammary glands were superficial cervical, cranial mediastinal, superficial inguinal and medial iliac. Differently, a previous lymphographic study by the same author identified only inguinal lymph nodes with blue dye in 9 healthy bitches and both ipsilateral inguinal and popliteal lymph nodes in one dog using fluorescein *(Pereira et al., 2003)*. In the same study, lymphatic pattern of neoplastic mammary glands was investigated using blue dye and reported draining nodes for the fourth mammary gland were the inguinal lymph center in 12 dogs and both the inguinal and axillary lymph nodes in 2 bitches. Similarly, a further study investigating the lymphatic drainage of neoplastic mammary glands using radiographic indirect lymphography, the identified lymph node of bitches with fourth mammary gland neoplasia were mostly the ipsilateral inguinal lymph nodes (7/9 cases) and in 2 cases both inguinal and axillary lymph nodes *(Patsikas et al., 2006)*. Therefore, for the caudal abdominal mammary gland, the most common draining lymph center is the inguinal, but contributes from superficial cervical, axillary, cranial mediastinal, medial iliac and popliteal lymph nodes have been described. Preliminary results of this study confirm the variability of forth mammary gland lymphatic pattern, whereas the contribute of inguinal lymph node was constantly identified by each technique in every case.
Beside the intrinsic fourth mammary glands drainage variance, in this study the identified SLNs differed between preoperative mapping modalities and between preoperative and intraoperative techniques. The reasons behind this discrepancy are not clear. The number of SLN identified with the radiotracer is greater in all the fourth mammary glands tumor cases compared to CT-indirect lymphography. A possible explanation could be the radiocolloid spill over from the SLN to the efferent second-echelon nodes. However, the same radiopharmaceutical has been used in the 2 dogs with tumor of the fifth mammary gland and only one lymph node was identified with all techniques. Regarding preoperative planar lymphoscintigraphy and intraoperative handheld gamma probe detection, the two differing

cases (dog n. 2 and n. 5) show a converse trend. In dog n.2, the intraoperative techniques found an additional draining node (axillary) which could have been missed in planar images. In fact, one of the greater drawbacks of planar lymphoscintigraphy is the lack of anatomical details and the "*shine-through*" effect from the injection site, which can challenge SLN identification, especially in cases of multiple nodal uptakes.

The differences observed in dog n. 5 (*Figure 4.1*) are more difficult to explain. CT-indirect lymphography identified 2 draining nodes, inguinal and medial iliac, while planar lymphoscintigraphy detected the ipsilateral axillary accessory as an additional node. Despite that, intraoperative gamma probe identified only the inguinal node. This is the only dogs that received surgery the day after preoperative lymphoscintigraphy. In author's experience, performing intraoperative SLN mapping the day after radiopharmaceutical injection never affected the intraoperative lymph node identification rate compared to preoperative lymphoscintigraphy. However, further studies are needed to prove this statement.

Preoperative lymphoscintigraphy combined with intraoperative mapping techniques is the gold standard for SLN detection in human oncology and has been successfully employed in dogs with different types of malignancies *(Balogh et al., 2002; Worley et al., 2012; Linden et al., 2019; Ferrari et al., 2020)*. However, lymphoscintigraphy is available in a limited number of veterinary facilities, due to the restrictions on radioactive material detention, use and disposal, and due to the high cost of the associated equipment. CT-indirect lymphography has gained more interest in veterinary medicine because of a wider availability of CT scans and a greater anatomical detail *(Soultani et al., 2016; Majeski et al., 2017; Rossi et al., 2018; Grimes et al., 2017; Randall et al., 2020; Grimes et al., 2020)*. Furthermore, CT offers the possibility to combine lymphatic mapping with contrast enhanced studies, which can provide valuable information for tumor staging. In this report, one dog enrolled in the study was excluded after contrast enhanced-CT images showed multiple musculoskeletal and hepatic neoformations cytologically compatible with epithelial neoplasia metastatic spread, proving the utility of this modality for tumor staging.

Because of the employment of different mapping techniques depending on their availability, their costs and upon clinician preferences, further experimental and clinical study are needed to investigate which technique more reliably identifies the true SLN in oncological veterinary practice. Despite the limited sample size, the preliminary results of this study showed discrepancies among the lymph nodes identified using different mapping techniques, particularly in the canine neoplastic fourth mammary gland. The use of a combined detection technique is thus of paramount importance in order to reduced false negative cases.

5. Conclusion

In oncological patients, the assessment of lymphatic metastatic spread is an essential component of the tumor staging process: the nodal status represents a significant prognostic factor and guides the choice of the optimal adjuvant treatment. Indeed, sampling the correct lymph node, i.e., the one that truly drains the tumor site, is crucial in order to reduce false-negative results and prevent the subsequent under-staging of the patient. This tumor-draining node represents the so called “sentinel lymph node”, which is considered the indicator of the systemic nodal histopathological status.

The results of our studies show that the SLN can be identified within unexpected lymphatic basins compared to anatomic regional lymph node, confirming the necessity to include the SLN mapping procedure in the staging of canine and feline oncological patients to overcome the individual variability of lymphatic drainage patterns increased by tumor-induced lymphangiogenesis.

Different modalities for SLN detection have been developed in human medicine and applied in veterinary oncology. Firstly, we investigate the use of lymphoscintigraphy - which is considered, to date, the gold standard in human oncology - in dogs with spontaneous malignant tumor and, for the first time, in a client own cat. This technique proved to be a feasible, safe and effective method for SLN mapping, focusing the surgical extirpation in a specific lymphocentrum. To improve the SLN identification rate and guide surgical dissection, we described a combined protocol including preoperative lymphoscintigraphy and intraoperative use of a handheld gamma probe and methylene blue dye.

Unexpectedly, the SLN mapping procedure in dogs with thyroid malignancies proved to be challenging in both the first and the second study, with alternate failing of preoperative and intraoperative techniques, despite previously reported success. Furthermore, the impact of previous surgery, radiotherapy and chemotherapy on canine lymphatic drainage and, consequently, on SLN mapping procedure is worth further investigation.

A recently proposed modality for SLN detection is SPECT/CT hybrid imaging, which is counted to provide both functional and anatomical data, increasing the SLN identification rate. In the second study, we report the feasibility of SPECT/CT images fusion with an opensource software (AMIDE) for SLN detection in dogs with different malignant tumors. The success of the images merging is strictly related to patients positioning, which could be further improved using external fiducial markers. In dogs where images fusion was accomplished, we observed a perfect agreement between the lymph nodes identified with planar lymphoscintigraphy and SPECT/CT images. The clinical relevance of SPECT/CT combined imaging modality for SLN mapping in veterinary oncology needs to be further evaluated, for example assessing its utility in surgical planning.

Nevertheless, a considerable limitation of lymphoscintigraphy is the restrictive access to radioactive tracers and the high cost of the equipment, which limit the number of veterinary facilities with nuclear medicine services. Computed tomography-indirect lymphography has progressively gained more interest in veterinary medicine because of a wider availability of

CT scans and a greater anatomical detail. In the third study we present an ongoing study comparing CT-indirect lymphography and lymphoscintigraphy for SLN mapping in dogs with mammary tumors. Despite the limited sample size, the preliminary results showed discrepancies among the lymph nodes identified using different mapping modalities, particularly in dogs presenting tumor at the fourth mammary gland. Therefore, as previously stated, the use of a combined detection technique is of paramount importance to improve SLN identification rate and reduce false-negative results.

6. Bibliography

1. **Alex JC**. The application of sentinel node radiolocalization to solid tumors of the head and neck: a 10-year experience. *Laryngoscope* 2004;1142-19.
2. **Balogh L**, Thuróczy J, Andócs G, et al. Sentinel lymph node detection in canine oncological patients. *Nucl Med Rev Cent East Eur*. 2002;5:139-144.
3. **Beer P**, Venzin C, Rohrer Bley C, et al. A comparison of near-infrared fluorescence imaging, lymphoscintigraphy and methylene blue dye method for intraoperative sentinel lymph node mapping in canine mast cell tumors: a prospective case series. Paper presented at: ECVS Annual Scientific Meeting 2019; July 2-4, 2019; Budapest, Hungary.
4. **Beserra HEO**, Grandi F, Dufloth RM, et al. Metastasis of mammary carcinoma in bitches: evaluation of the sentinel lymph node technique. *Advances in Breast Cancer Research*. 2016;5(02):58-65.
5. **Brissot HN**, Edery EG. Use of indirect lymphography to identify sentinel lymph node in dogs: a pilot study in 30 tumours. *Vet Comp Oncol*. 2016;15(3): 740-753.
6. **Cabañas RM**. An approach for the treatment of penile carcinoma. *Cancer*. 1977;39:456-466.
7. **Cabon Q**, Sayag D, Texier I, et al. Evaluation of intraoperative fluorescence imaging-guided surgery in cancer-bearing dogs: a prospective proof-of-concept phase II study in 9 cases. *Transl Res*. 2016;170:73-88.
8. **Choi M**, Yoon J, Choi M. Contrast-enhanced ultrasound sonography combined with strain elastography to evaluate mandibular lymph nodes in clinically healthy dogs and those with head and neck tumors. *The Vet Journ*, 2020;*257*:105447.
9. **Dogan NU**, Dogan S, Favero G, et al. The basics of sentinel lymph node biopsy: anatomical and pathophysiological considerations and clinical aspects. *J Oncol*. 2019;3415630.
10. **Erba PA**, Bisogni G, Del Guerra A, Mariani G. Methodological Aspects of Lymphoscintigraphy: Radiopharmaceuticals and Instrumentation. In: *Atlas of Lymphoscintigraphy and Sentinel Node Mapping*, pp. 17-25. 2013, Springer, Milano.
11. **Even-Sapir E**, Lerman H, Lievshitz G, et al. Lymphoscintigraphy for sentinel node mapping using a hybrid SPECT/CT system. *J Nucl Med*. 2003;44: 1413-1420.
12. **Eward WC**, Mito JK, Eward CA, et al. A novel imaging system permits real-time in vivo tumor bed assessment after resection of naturally occurring sarcomas in dogs. *Clin Orthop Relat Res*. 2013;471(3):834-842.
13. **Favril S**, Stock E, Hernot S, et al. Sentinel lymph node mapping by near-infrared fluorescence imaging and contrast-enhanced ultrasound in healthy dogs. *Vet Comp Oncol*. 2019;17:89-98.
14. **Ferrari R**, Chiti LE, Manfredi M, et al. Biopsy of sentinel lymph nodes after injection of methylene blue and lymphoscintigraphic guidance in 30 dogs with mast cell tumors. *Vet*

Surg. 2020;49(6):1099-1108

15. **Fidel J**, Kennedy KC, Dernell WS, et al. Preclinical validation of the utility of BLZ-100 in providing fluorescence contrast for imaging spontaneous solid tumors. *Cancer Res*. 2015;75(20):4283–4291.
16. **Fidler IJ**. The pathogenesis of cancer metastasis: the "seed and soil" hypothesis revisited. *Nat Rev Cancer*. 2003;3:453-458.
17. **Fournier Q**, Cazzini P, Bavcar S, et al. Investigation of the utility of lymph node fine-needle aspiration cytology for the staging of malignant solid tumors in dogs. *Vet Clin Pathol*. 2018;47:489-500.
18. **Fournier Q**, Thierry F, Longo M, et al. Contrast-enhanced ultrasound for sentinel lymph node mapping in the routine staging of canine mast cell tumours: A feasibility study. *Vet Comp Oncol*. 2020;1–12
19. **Friedl P**, Wolf K. Tumour-cell invasion and migration: diversity and escape mechanisms. *Nat Rev Cancer*. 2003;3(5):362–374.
20. **Garbay J**, Skalli-Chrisostome D, Leymarie N, et al. The Role of Blue Dye in Sentinel Node Detection for Breast Cancer: A Retrospective Study of 203 Patients. *Breast Care*. 2016;11:128-132.
21. **Gelb HR**, Freeman LJ, Rohleder JJ, Snyder PW. Feasibility of contrast-enhanced ultrasound-guided biopsy of sentinel lymph nodes in dogs. *Vet Radiol Ultrasound*. 2010;51(6):628-633.
22. **Gelmini R**, Campanelli M, Cabry F, et al. Role of sentinel node in differentiated thyroid cancer: a prospective study comparing patent blue injection technique, lymphoscintigraphy and the combined technique. *J Endocrinol Invest*. 2018;41(3):363-370.
23. **Gould EA**, Winship T, Philbin PH, Kerr HH. Observations on a 'sentinel node' in cancer of the parotid. *Cancer.* 1960;13:77-78.
24. **Griffin L**, Frank CB, Seguin B. Pilot study to evaluate the efficacy of lymphotropic nanoparticle enhanced MRI for diagnosis of metastatic disease in canine head and neck tumours. *Vet Comp Oncol*. 2019;1-8.
25. **Grimes JA**, Secrest SA, Northrup NC, et al. Indirect computed tomography lymphangiography with aqueous contrast for evaluation of sentinel lymph nodes in dogs with tumors of the head. *Vet Radiol Ultrasound*. 2017;58:559-564.
26. **Grimes JA**, Secrest SA, Wallace ML, et al. Use of indirect computed tomography lymphangiography to determine metastatic status of sentinel lymph nodes in dogs with a pre-operative diagnosis of melanoma or mast cell tumour. *Vet Comp Oncol*. 2020;1-7.
27. **Guermazi A**, Brice P, Hennequin C, Sarfati E. Lymphography: an old technique retains its usefulness. *Radiographics*, 2003;23(6):1541-1558.
28. **Haers H**, Saunders JH. Review of clinical characteristics and applications of contrast-enhanced ultrasonography in dogs. *J Am Vet Med Assoc*. 2009;234(4):460-470.

29. **Hayashi H**, Tangoku A, Suga K, et al. CT lymphography-navigated sentinel lymph node biopsy in patients with superficial esophageal cancer. *Surgery*. 2006;139(2):224-235.
30. **Hlusko KC**, Cole R, Tillson DM, et al. Sentinel lymph node detection differs when comparing lymphoscintigraphy to lymphography using water soluble iodinated contrast medium and digital radiography in dogs. *Vet Radiol Ultrasound*. 2020;1-8.
31. **Hlusko KC**, Cole R, Tillson DM, et al. The effect of surgery on lymphoscintigraphy drainage patterns from the canine brachium in a simulated tumor model. *Vet Surg*. 2020;49:1118-1124.
32. **IAEA**, International atomic energy agency. "Technetium-99m Radiopharmaceuticals: Status and Trends."Radioisotopes and Radiopharmaceuticals Series No.1, Vienna 2009.
33. **Inubushi M**, Tatsumi M, Yamamoto Y, et al. European research trends in nuclear medicine. *Ann Nucl Med*. 2018;32:579-82.
34. **Keshtgar MR**, Ell PJ. Sentinel lymph node detection and imaging. *Eur J Nucl Med*. 1999;26(1):57-67.
35. **Kim H**, Lee SK, Kim YM, et al. Fluorescent iodized emulsion for pre- and intraoperative sentinel lymph node imaging: validation in a pre-clinical model. *Radiology*. 2015;275(1):196-204.
36. **Kizu H**, Takayama T, Fukuda M, et al. Fusion of SPECT and multidetector CT images for accurate localization of pelvic sentinel lymph nodes in prostate cancer patients. *J Nucl Med Technol.* 2005;33:78-82.
37. **Knapp DW**, Adams LG, Degrand AM, et al. Sentinel lymph node mapping of invasive urinary bladder cancer in animal models using invisible light. *Eur Urol*. 2007;52(6):1700-1708.
38. **Kolbeck KJ**. Lipiodol=Ethiodol. *J Vasc Interv Radiol*. 2011;3(22):419-420.
39. **Kosaka N**, Ogawa M, Choyke PL, Kobayashi H. Clinical implications of near-infrared fluorescence imaging in cancer. *Future oncology*. 2009;5(9):1501-1511.
40. **Langenbach A**, McManus PM, Hendrick MJ, et al. Sensitivity and specificity of methods of assessing the regional lymph nodes for evidence of metastasis in dogs and cats with solid tumours. *JAVMA*. 2001;218:1424-1428.
41. **Lee AC**, Keshtgar MRS, Waddington WA, Ell PJ. (2002). The role of dynamic imaging in sentinel lymph node biopsy in breast cancer. *Eur J Cancer*. 2002;38(6):784-787.
42. **Lerman H**, Metser U, Lievshitz G, et al. Lymphoscintigraphic sentinel node identification in patients with breast cancer: the role of SPECT-CT. *Eu J Nucl Med Mol Imaging*, 2006:33(3);329-337.
43. **Li J**, Chen X, Qi M, Li Y. Sentinel lymph node biopsy mapped with methylene blue dye alone in patients with breast cancer: A systematic review and meta-analysis. *PLoS ONE* 2018;13(9):e0204364.
44. **Lim JS**, Choi J, Song J, et al. Nanoscale iodized oil emulsion: a useful tracer for pretreatment sentinel node detection using CT lymphography in a normal canine gastric model. *Surg Endosc*. 2012;26(8):2267-2274.

45. **Linden DS**, Cole R, Tillson DM, et al. Sentinel lymph node mapping of the canine anal sac using lymphoscintigraphy: A pilot study. *Vet Radiol Ultrasound*. 2019;60:346-350
46. **Liptak JM**, Boston SE. Nonselective lymph node dissection and sentinel lymph node mapping and biopsy. *Vet Clin North Am Small Anim Pract*. 2019;49:793-807.
47. **Liss MA**, Stroup SP, Qin Z, et al. Robotic-assisted fluorescence sentinel lymph node mapping using multimodal image guidance in an animal model. *Urology*. 2014;84(4):982.e9-982.14.
48. **Lissidini G**, Trifirò G, Veronesi P, et al. Could radiotherapy play a major role in misidentification of sentinel lymph node in breast cancer recurrence? *Radiother Oncol*, 2019;131:237-238.
49. **Loening AM**, Gambhir SS. AMIDE: A completely free system for medical imaging data analysis. *J Nucl Med*. 2001;42(5):192P.
50. **Loening AM**, Gambhir SS. AMIDE: A Free Software Tool for Multimodality Medical Image Analysis. *Molec Imag.* 2003;2(3):131-137.
51. **Lurie DM**, Seguin B, Schneider PD, et al. Contrast-assisted ultrasound for sentinel lymph node detection in spontaneously arising canine head and neck tumors. *Invest Radiol*. 2006;41(4):415-421.
52. **Lyman GH**, Somerfield MR, Bosserman LD, et al. Sentinel lymph node biopsy for patients with early-stage breast cancer: American Society of Clinical Oncology clinical practice guideline update. *J Clin Oncol*. 2017;35(5):561-564.
53. **Majeski SA**, Steffey MA, Fuller M, et al. Indirect computed tomographic lymphography for iliosacral lymphatic mapping in a cohort of dogs with anal sac gland adenocarcinoma: technique description. *Vet Radiol Ultrasound*. 2017;58: 295-303.
54. **Manca G**, Rubello D, Tardelli E, et al. Sentinel lymph node biopsy in breast cancer: indications, contraindications, and controversies. *Clin Nucl Med*. 2016;41(2):126-133.
55. **Marconato L**, Polton G, Stefanello D, et al. Therapeutic impact of regional lymphadenectomy in canine stage II cutaneous mast cell tumours. *Vet Comp Oncol*. 2018;16:580-589.
56. **Marconato L**, Stefanello D, Kiupel M, et al. Adjuvant medical therapy provides no therapeutic benefit in the treatment of dogs with low-grade mast cell tumours and early nodal metastasis undergoing surgery. *Vet Comp Oncol*. 2020;1-7.
57. **Mathelin C**, Croce S, Brasse D, et al. Methylene blue dye, an accurate dye for sentinel lymph node identification in early breast cancer. *Anticancer research*. 2009;29(10): 4119-4125
58. **Mayer MN**, Kraft SL, Bucy DS, et al. Indirect magnetic resonance lymphography of the head and neck of dogs using Gadofluorine M and a conventional gadolinium contrast agent: a pilot study. *Can Vet J*. 2012;53(10):1085-1090.
59. **Mayer MN**, Silver TI, Lowe CK, Anthony JM. Radiographic lymphangiographyin the dog using iodized oil. *Vet Comp Oncol*. 2013;11(2):151-161.
60. **Misselwitz B**, Platzek J, Radüchel B, et al. Gadofluorine 8: Initial experience with a new

contrast medium for interstitial MR lymphography. *MAGMA* 1999;8:190-195.

61. **Moody AN**, Bull J, Culpan AM, et al. Preoperative sentinel lymph node identification, biopsy and localisation using contrast enhanced ultrasound (CEUS) in patients with breast cancer: a systematic review and meta-analysis. *Clin Radiol*. 2017;72(11):959-971.
62. **Morton DL**, Wen DR, Wong JH, et al. Technical details of intraoperative lymphatic mapping for early stage melanoma. *Archives of surgery*. 1992;127(4): 392-399.
63. **Naaman Y**, Pinkas L, Roitman S, et al. The added value of SPECT/CT in sentinel lymph nodes mapping for endometrial carcinoma. *Ann Surg Oncol*. 2016;23(2):450-455.
64. **Nakagawa M**, Morimoto M, Takechi H, et al. Preoperative diagnosis of sentinel lymph node (SLN) metastasis using 3D CT lymphography (CTLG). *Breast Cancer.* 2016;23:519-524.
65. **Niebling MG**, Pleijhuis RG, Bastiaannet E, et al. A systematic review and meta-analyses of sentinel lymph node identification in breast cancer and melanoma, a plea for tracer mapping. *Eur J Surg Oncol*. 2016;42(4):466-473.
66. **Nowikiewicz T**, Głowacka-Mrotek I, Tarkowska M, et al. Failure of sentinel lymph node mapping in breast cancer patients qualified for treatment sparing axillary lymph nodes. *Breast J*. 2020;26(5):873-881.
67. **Nwogu CE**, Kanter PM, Anderson TM. Pulmonary lymphatic mapping in dogs: use of technetium sulfur colloid and isosulfan blue for pulmonary sentinel lymph node mapping in dogs. *Cancer Invest.* 2002;20(7-8):944-947.
68. **Papadopoulou PL**, Patsikas MN, Charitanti A, et al. The lymph drainage pattern of the mammary glands in the cat: a lymphographic and computerized tomography lymphographic study. *Anat, Histol, Embryol*. 2009;38(4), 292-299.
69. **Patsikas MN**, Dessiris A. The lymph drainage of the mammary glands in the bitch: a lymphographic study. Part I: The 1st, 2nd, 4th and 5th mammary glands. *Anat, Histol, Embryol*. 1996;25(2):131-138.
70. **Patsikas MN**, Dessiris A. The lymph drainage of the mammary glands in the bitch: a lymphographic study. Part II: the 3rd mammary gland. *Anat, Histol, Embryol*. 1996;25(2): 139-143.
71. **Patsikas MN**, Karayannopoulou M, Kaldrymidoy E, et al. The lymph drainage of the neoplastic mammary glands in the bitch: a lymphographic study. *Anat, Histol, Embryol*. 2006;35(4):228-234.
72. **Patsikas MN**, Papadopoulou PL, Charitanti A, et al. Computed tomography and radiographic indirect lymphography for visualization of mammary lymphatic vessels and the sentinel lymph node in normal cats. *Vet Radiol Ultrasound*. 2010;51(3):299-304.
73. **Pereira CT**, Luiz Navarro Marques F, Williams J, et al. 99mTc-labeled dextran for mammary lymphoscintigraphy in dogs. *Vet Radiol Ultrasound*. 2008;49(5):487-491.
74. **Pereira CT**, Rahal SC, de Carvalho Balieiro JC, Ribeiro AACM. Lymphatic drainage on healthy and neoplasic mammary glands in female dogs: can it really be altered?. *Anat, Histol, Embryol*. 2003;32(5):282-290.

75. **Pinheiro LG**, Oliveira Filho RS, Vasques PH, et al. Hemosiderin: a new marker for sentinel lymph node identification. *Acta Cir Bras*. 2009;24(6):432–436.
76. **Ran S**, Volk L, Hall K, Flister MJ. Lymphangiogenesis and lymphatic metastasis in breast cancer. *Pathophysiology*. 2010;17(4): 229-251.
77. **Randall EK**, Jones MD, Kraft SL, Worley DR. The development of an indirect computed tomography lymphography protocol for sentinel lymph node detection in head and neck cancer and comparison to other sentinel lymph node mapping techniques. *Vet Comp Oncol*. 2020;1-11.
78. **Reynolds JS**, Troy TL, Mayer RH, et al. Imaging of spontaneous canine mammary tumors using fluorescent contrast agents. *Photochem Photobiol* 1999;70:87-94.
79. **Riveros M**, Garcia R, Cabañas R. Lymphadenography of the dorsal lymphatics of the penis. Technique and results. *Cancer*. 1967;20(11):2026-2031.
80. **Rossi F**, Körner M, Suárez J, et al. Computed tomographic-lymphography as a complementary technique for lymph node staging in dogs with malignant tumors of various sites. *Vet Radiol Ultrasound*. 2018;59:155-162.
81. **Sautet JY**, Rubert J, Lopez C, et al. Lymphatic system of mammary glands in the dog: an approach to the surgical treatment of malignance tumors. *Canine Pract*. 1992;17:30-33.
82. **Scherern K**, Studer W, Figueiredo V, Bircher AJ. Anaphylaxis to isosulfan blue and cross-reactivity to patent blue V: case report and review of the nomenclature of vital blue dyes. *Annals of Allergy, Asthma & Immunology*. 2006;96(3):497-500.
83. **Siddique M**, Nawaz MK, Bashir H. The usefulness of SPECT/CT in sentinel node mapping of early stage breast cancer patients showing negative or equivocal findings on planar scintigraphy. *Asia Ocean J Nucl Med Biol*. 2018;6(2):80-89.
84. **Soultani C**, Patsikas MN, Karayannopoulou M, et al. Assessment of sentinel lymph node metastasis in canine mammary gland tumors using computed tomographic indirect lymphography. *Vet Radiol Ultrasound*. 2016;58:186-196.
85. **Stacker SA**, Williams SP, Karnezis T, et al. Lymphangiogenesis and lymphatic vessel remodelling in cancer. *Nature Reviews Cancer*. 2014;14(3):159-172.
86. **Suami H**, Yamashita S, Soto-Miranda MA, Chang DW. Lymphatic territories (lymphosomes) in a canine: an animal model for investigation of postoperative lymphatic alterations. *PLoS One*. 2013;8(7):e69222.
87. **Suga K**, Karino Y, Fujita T, et al. Cutaneous drainage lymphatic map with interstitial multidetector-row computed tomographic lymphography using iopamidol: preliminary results. *Lymphology*. 2007;40(2);63-73.
88. **Suga K**, Yuan Y, Ueda K, et al. Computed tomography lymphography with intrapulmonary injection of iopamidol for sentinel lymph node localization. *Invest Radiol*. 2004;39(6):313-324.
89. **Suga K[a]**, Ogasawara N, Yuan Y, et al. Visualization of breast lymphatic pathways with an indirect computed tomography lymphography using a nonionic monometric contrast

medium iopamidol: preliminary results. *Invest Radiol*. 2003; 38(2):73-84.

90. **Suga K[b]**, Ogasawara N, Okada M, Matsunaga N. Interstitial CT lymphography-guided localization of breast sentinel lymph node: preliminary results. *Surgery*. 2003;133(2):170-179.
91. **Suga K[c]**, Yuan Y, Ogasawara N, Whitman GJ. Localization of breast sentinel lymph nodes by MR lymphography with a conventional gadolinium contrast agent: preliminary observations in dogs and humans. *Acta Radiol*. 2003;44:35-42
92. **Tada K**, Nishimura S, Miayagi Y, et al. The effect of an old surgical scar on sentinel node mapping in patients with breast cancer: a report of five cases. *Eur J of Surg Oncol*. 2005;31:840-844.
93. **Tardelli E**, Mazzarri S, Rubello D, et al. Sentinel lymph node biopsy in cutaneous melanoma. *Clin Nucl Med*. 2016;41(12):e498-e507.
94. **Townsend KL**, Milovancev M, Bracha S. Feasibility of near-infrared fluorescence imaging for sentinel lymph node evaluation of the oral cavity in healthy dogs. *Am J Vet Res*. 2018;79(9):995-1000.
95. **Tuohy JL**, Milgram J, Worley DR, Dernell WS. A review of sentinel lymph node evaluation and the need for its incorporation into veterinary oncology. *Vet Comp Oncol*. 2009;7(2): 81-91.
96. **Tuohy JL**, Worley DR. Pulmonary lymph node charting in normal dogs with blue dye and scintigraphic lymphatic mapping. *Res Vet Sci*, 2014;97(1):148-155.
97. **Turkbey B**, Hoyt RF, Agarwal HK, et al. Magnetic resonance sentinel lymph node imaging of the prostate with gadofosveset trisodium-albumin: preliminary results in a canine model. *Acad Radiol*. 2015;22(5):646-652.
98. **Uren RF**, Howman-Giles R, Chung D, Thompson JF. Imaging sentinel lymph nodes. *The Cancer Journal.* 2015;21(1): 25-32.
99. **van Manen L**, Handgraaf HJM, Diana M, et al. A practical guide for the use of indocyanine green and methylene blue in fluorescence-guided abdominal surgery. *J Surg Oncol*. 2018;118:283-300.
100. **Van SL**. ^{99m}Tc generator development: up-to-date ^{99m}Tc recovery technologies for increasing the effectiveness of ^{99}Mo utilization. *Sci Technol Nucl Install* 2014;e345252:1
101. **Vasques PHD**, Pinheiro LGP, Torres-de-Melo JRDM, et al. The impact of previous para-areolar incision in the upper outer quadrant of the breast on the localization of the sentinel lymph node in a canine model. *Clinics*. 2011;66(8):1413-1418.
102. **Wagner T**, Buscombe J, Gnanasegaran G, Navalkissoor S. SPECT/CT in sentinel node imaging. *Nucl Med Commun*. 2013;34(3):191-202.
103. **Wang Y**, Cheng Z, Li J, Tang J. Gray-scale contrast-enhanced ultrasonography in detecting sentinel lymph nodes: an animal study. *Eur J Radiol*. 2010;74(3):e55-e59.
104. **Weishaar KM**, Thamm DH, Worley DR, Kamstock DA. Correlation of nodal mast cell with clinical outcome in dogs with mast cell tumour and a proposed classification system for the evaluation of node metastasis. *J Comp Pathol*. 2014;151(4): 329-338.

105. **Wells S**, Bennett A, Walsh P, et al. Clinical usefulness of intradermal fluorescein and patent blue violet dyes for sentinel lymph node identification in dogs. *Vet Comp Oncol*. 2006;4(2): 114-122.

106. **Williams LE**, Packer RA. Association between lymph node size and metastasis in dogs with oral malignant melanoma: 100 cases (1987–2001). *JAVMA*. 2003;222(9):1234-1236.

107. **Wisner ER**, Katzberg RW, Kobik PD, et al .Iodinated nanoparticles for indirect computed tomography lymphography of the craniocervical and thoracic lymph nodes in normal dogs. *Acad Radiol*. 1994;1:377-384.

108. **Wong JH**, Cagle LA, Morton, DL. Lymphatic drainage of skin to a sentinel lymph node in a feline model. *Ann Surg*. 1991;214(5):637-641.

109. **Worley DR**. Incorporation of sentinel lymph node mapping in dogs with mast cell tumours: 20 consecutive procedures. *Vet Comp Oncol*. 2012;12(3): 215-226.